THESIS

SELENIUM TRANSPORT IN PLANTS WITH A SPECIAL FOCUS ON SELENIUM HYPERACCUMULATORS

Submitted by

Richard Croxall Trippe III

Department of Biology

In partial fulfillment of the requirements

For the Degree of Master of Science

Colorado State University

Fort Collins, Colorado

Fall 2021

Master's Committee:

Advisor: Elizabeth Pilon-Smits
Co-Advisor: Marinus Pilon

Christie Peebles
Michela Schiavon

ABSTRACT

SELENIUM TRANSPORT IN PLANTS WITH A SPECIAL FOCUS

ON SELENIUM HYPERACCUMULATORS

The aims of this thesis are to synthesize current knowledge of selenium (Se) transport and metabolism in plants and improve understanding of Se transport in a class of plant species known as Se hyperaccumulators (HAs). These Se HAs can accumulate Se at up to 1,000 times higher concentrations than normal plants by utilizing specialized systems of Se transport and metabolism.

The first chapter of this thesis constitutes a review of the current knowledge about Se transport and metabolism in plants, with a focus on implications for biofortification and phytoremediation. Selenium is a necessary human micronutrient, and around a billion people worldwide may be Se deficient. This can be ameliorated by Se biofortification of staple crops. Selenium is also a potential toxin at higher concentrations, and multiple environmental disasters over the past 50 years have been caused by Se pollution from agricultural and industrial sources. Phytoremediation by plants able to take up large amounts of Se is an important tool to combat pollution issues. Both biofortification and phytoremediation applications require a thorough understanding of how Se is taken up and metabolized by plants. Selenium uptake and translocation in plants is largely accomplished via sulfur (S) transport proteins. Current understanding of these transporters is reviewed here, and transporters that may be manipulated to improve Se uptake are discussed. Plant Se metabolism also largely follows the S metabolic pathway. This pathway is reviewed here, with special focus on genes that may be manipulated to

reduce the accumulation of toxic metabolites or enhance the accumulation of nontoxic metabolites. Finally, unique aspects of Se transport and metabolism in Se HAs are reviewed. Selenium hyperaccumulation mechanisms and potential applications of these mechanisms to biofortification and phytoremediation are presented.

The second chapter of this thesis covers the results of experimental studies expressing putative Se HA transporter proteins in a yeast (*Saccharomyces cerevisiae*) model system. Selenium hyperaccumulators are able to take up Se from the soil at concentrations many times higher than other native vegetation. Hyperaccumulators also show evidence of enhanced Se-specificity relative to sulfur. The mechanism for this Se specificity is investigated in this study. We hypothesize that in hyperaccumulators one or more sulfate transport proteins has evolved greater preference for the Se analog, selenate. This study focuses on putative root-to-shoot sulfate/selenate transport proteins SpSULTR2;1 and SpSULTR3;5 from Se hyperaccumulator *Stanleya pinnata* (Brassicaceae). The coding regions of these genes were amplified via reverse transcription polymerase chain reaction (RT-PCR), cloned in a yeast expression vector and sequenced. SpSULTR2;1 and SpSULTR3;5 were found to be 678 and 638 amino acids in length, respectively. Both proteins showed the characteristic N-terminal cytosolic domain, 12 membrane-spanning domains, and C-terminal cytosolic STAS (Sulphate Transporter and Anti-Sigma factor antagonist) domains. SpSULTR2;1 and SpSULTR3;5 were assayed for selenate specificity by quantifying their relative selenate and sulfate uptake capacities in baker's yeast (*Saccharomyces cerevisiae*). This assay was complemented with selenate-dependent growth curves in liquid media and a selenate tolerance assay on solid media. Both SpSULTR2;1 and SpSULTR3;5 were expressed by the yeast cells, determined by dot-blot immunoassay. Expression of SpSULTR2;1 effected a slight but non-significant increase in the Se concentration

in the yeast relative to the empty vector control in a 1-hour uptake assay when exposed to 1 mM selenate, but not when exposed to 0.1 mM selenate. SpSULTR3;5 was not able to increase the selenate concentration in the yeast relative to the control in the uptake assay. Yeast expressing SpSULTR2;1 or SpSULTR3;5 demonstrated similar selenate tolerance to empty-vector controls. Expression of SpSULTR3;5 or SpSULTR2;1 also did not significantly affect growth relative to the control in liquid media. In conclusion, more studies are needed to determine with certainty whether SpSULTR2;1 or SpSULTR3;5 have selenate-specific transport capability.

ACKNOWLEDGEMENTS

First and foremost, I want to thank my dedicated advisor, Dr. Elizabeth Pilon-Smits, who patiently guided me. I feel extremely lucky to have had such a supportive and knowledgeable advisor. Thanks also to my co-advisor Dr. Marinus Pilon, who provided invaluable guidance and support, as well as to my committee members for their support and advice: Dr. Christie Peebles and Dr. Michela Schiavon. Of course, I also must thank all my lab mates—Leonardo Lima, Cameron Hunter, Sue Abernathy, and Gretchen Kroh—for all their help and support. Thanks also to other past Pilon/Pilon-Smits lab graduate students for building the foundations without which my research would not have been possible. I would also like to acknowledge the Biology Department and specifically the Stavros Family Fund for their financial support. Finally, I never could have completed this degree without the constant support and encouragement of both my parents, Rich and Beth Trippe, and my fiancé, Alison Post.

DEDICATION

To Alison,

who helped me believe I could do it.

TABLE OF CONTENTS

CHAPTER 1: SELENIUM TRANSPORT AND METABOLISM IN PLANTS: PHYTOREMEDIATION AND BIOFORTIFICATION IMPLICATIONS

1.1 Summary

The aim of this review is to synthesize current knowledge of selenium (Se) transport and metabolism in plants, with a focus on implications for biofortification and phytoremediation. Selenium is a necessary human micronutrient, and around a billion people worldwide may be Se deficient. This can be ameliorated by Se biofortification of staple crops. Selenium is also a potential toxin at higher concentrations, and multiple environmental disasters over the past 50 years have been caused by Se pollution from agricultural and industrial sources. Phytoremediation by plants able to take up large amounts of Se is an important tool to combat pollution issues. Both biofortification and phytoremediation applications require a thorough understanding of how Se is taken up and metabolized by plants. Selenium uptake and translocation in plants is largely accomplished via sulfur (S) transport proteins. Current understanding of these transporters is reviewed here, and transporters that may be manipulated to improve Se uptake are discussed. Plant Se metabolism also largely follows the S metabolic pathway. This pathway is reviewed here, with special focus on genes that may be manipulated to reduce the accumulation of toxic metabolites or enhance the accumulation of nontoxic metabolites. Finally, unique aspects of Se transport and metabolism in Se hyperaccumulators are reviewed. Hyperaccumulators, which can accumulate Se at up to 1,000 times higher concentrations than normal plants, present interesting specialized systems of Se transport and metabolism. Selenium hyperaccumulation mechanisms and potential applications of these mechanisms to biofortification and phytoremediation are presented.

1.2 Introduction

The element selenium (Se) is an essential factor in the structure of organic life. Many life forms, including humans, require Se in trace amounts because it is a necessary component of the amino acid selenocysteine (SeCys). Selenocysteine is often called the 21st protein amino acid due to its relative rarity—most species that require Se have between 1 and 30 proteins with a SeCys residue, typically in the active site (Zhang and Gladyshev, 2009). Humans have 25 known selenoproteins with a wide range of functions and consequent health effects. For example, the glutathione peroxidases function to scavenge free radicals and remove other oxidative damage-causing species (Rayman, 2012). The health effects of this class of selenoproteins include improved immune function, gastrointestinal and thyroid protection, and normal spermatogenesis (Rayman, 2012; Schmidt and Simonović, 2012). Although the functions of some human selenoproteins remain unknown (Regina et al., 2016), it is clear that selenoproteins on the whole are critical, because a complete lack of Se from the proteome is lethal (Bosl et al., 1997).

The United States Recommended Dietary Allowance for Se in adults is 55-75 μg/day (National Academy of Sciences, 2000). The amount of Se available for human consumption is ultimately dependent on the concentration of available Se in the local soil and the amount that edible plants are able to extract from this soil (Combs, 2001). Plants do not appear to require Se themselves (Zhang and Gladyshev, 2009), although in low concentrations Se has beneficial effects on plants including increased growth, antioxidative capacity, and resistance to biotic stresses (Pilon-Smits et al., 2009). In fact, any Se plants may contain is likely taken up non-specifically through the action of transport proteins for other nutrients, particularly sulfur (S) (Anderson, 1993). The Se content of human diets can vary widely, depending largely on the concentration of available Se in the soil of the region. Since Se-poor soils are found in populous

regions worldwide (including parts of China, Siberia, Scandinavia, sub-Saharan Africa, and New Zealand), Se deficiency may affect as many as one billion people (Combs, 2001).

Selenium deficiency, like other micronutrient deficiencies, manifests subtly. It is linked to increased susceptibility to infections (including COVID-19 and HIV), cancers (especially colorectal) and other diseases (Hoffmann and Berry, 2008; Zhang et al., 2020). There is also evidence that selenoprotein PHGPx, a glutathione peroxidase, is essential to sperm motility, and therefore male fertility (Ursini et al., 1999). Furthermore, Se deficiency can mimic the effects of iodine deficiency, leading to hypothyroidism (Arthur et al., 1992). The obscure yet debilitating effects of Se and other micronutrient deficiencies has earned them the collective appellation of "hidden hunger" (de Valença et al., 2017).

On the other end of the spectrum, selenosis—the condition caused by excessive Se—is as dangerous as Se deficiency. Chronic selenosis occurs when individuals ingest excess Se for long periods of time, at levels that are not high enough to cause immediate symptoms. The classic signs of chronic selenosis in humans are hair loss, nail damage, and rash. However, a range of other symptoms have been attributed to chronic selenosis, including various nervous and endocrine system effects, as well as increased risk of some cancers and type 2 diabetes (Vinceti et al., 2017; World Health Organization, 1996). Though it is rarer than Se deficiency, there have been incidences of chronic selenosis in recent history, such as the documented cases in Enshi, China between 1958 and 1963 (Huang et al., 2013) and in Punjab, India between 1997 and 1998 (Hira et al., 2004). Acute selenosis can also occur in humans, as in several cases stemming from the ingestion of Se-rich chemical products such as gun bluing agents and excessive quantities of dietary supplements. Such cases, depending on the dose of Se ingested, present symptoms

ranging from those of chronic selenosis to organ failure and death (MacFarquhar et al., 2010; Matoba et al., 1986; See et al., 2006).

Excess Se is dangerous to other animal species as well. Environmental Se contamination from industrial and agricultural activities has caused selenosis outbreaks in various species in recent decades. The release of Se into sensitive waterways is often the origin of the contamination. For example, during the 1980s in the San Joaquin Valley of California, USA, Se-rich drainage water from irrigated farms was diverted to maintain marshland in the Kesterson Reservoir. This marsh, part of the Pacific Flyway, served as a critical waterfowl wintering and nesting site. A study of birds collected there between 1983 and 1985 found that tissue Se concentrations were many times higher than normal, correlating to reduced body weight, feather loss, and other signs of poor physical condition. Moreover, many dead or moribund birds at the site were determined to have suffered from Se toxicosis (Ohlendorf et al., 1990). In another case study in Western Colorado, USA, runoff from naturally Se-rich farmland over many years led to chronically elevated Se levels in the Colorado River, negatively affecting the survival of several native fish species (Hamilton, 1999). Similar stories of anthropogenic Se contamination continue to arise. Se contamination from both agricultural and oil refinery effluents has long been a cause for concern in the San Francisco Bay-Delta (Presser and Luoma, 2006). In a 2020 study of Se toxicity in minnows from the Bay-Delta area, at least 75% of minnows sampled demonstrated spinal deformities, which were linked to Se accumulation from both maternal tissues transferred to the offspring and feeding on contaminated prey (Johnson et al., 2020). Various mining industries also contribute to Se pollution, as for example when rainwater leaches Se from the exposed ash waste generated from coal-burning power plants (Khamkhash et al., 2017).

The effects of Se on ecological and human systems share an important commonality: plants can be strategically utilized to mitigate the degree to which Se impacts both systems. Human consumption of Se can be increased by planting crops which are bred or engineered to take up more Se from the soil. Similarly, planting Se-contaminated areas with species which can tolerate and accumulate nontoxic forms of Se can reduce the soil Se load, and therefore mitigate the amount of Se runoff into waterways. Therefore, this review places the current understanding of plant Se biology into the context of these major issues. Section 1.3 covers Se uptake and translocation in plants and describes how this information can be used to breed Se-fortified crops to supplement diets in Se-poor communities. Section 1.4 describes plant Se metabolism, toxicity, and tolerance. In this section, metabolic reactions which produce detoxified selenocompounds are highlighted as potentially valuable mechanisms for the phytoremediation of Se-contaminated soils. Section 1.5 discusses Se hyperaccumulators (HAs), a class of plants which is able to accumulate and tolerate concentrations of Se approximately 1,000 times higher than normal plants. Special attention is given to mechanisms of Se transport and metabolism which may enable this unique phenotype, because those mechanisms are instructive for both biofortification and phytoremediation purposes.

1.3 Selenium Uptake and Translocation in Plants

Selenate (SeO_4^{2-}) and selenite (SeO_3^{2-}) are the two major forms of bioavailable Se in soil, with selenate predominating in oxic soils and selenite predominating in anoxic soils (White, 2018). Organic selenocompounds like selenoamino acids are also present in significant concentrations in some soils (Abrams et al., 1990; El Mehdawi et al., 2015a) and can be imported by plant roots (Kikkert and Berkelaar, 2013). Plants are capable of taking up both sulfate and selenate ions at the root; however, neither ion is taken up through a Se-specific

transporter. Selenate is taken up via sulfate transporters (SULTRs), and selenite is taken up by phosphate transporters and aquaporins (Schiavon and Pilon-Smits, 2017; White, 2018). Selenite is quickly metabolized upon uptake. Selenate, however, can be found throughout the plant (Huang et al., 2017). The conventional assumption is that various SULTRs are responsible for this distribution of selenate (Anderson, 1993). After discussing Se uptake in Section 1.3.1, Section 1.3.2 reviews selenate translocation to the various plant tissues. Note that, although there are no alternative theories for the transport of selenate, there is also no concrete evidence to support the hypothesis that SULTRs are solely responsible for selenate movement within the plant. Next, Section 1.3.3 discusses the plant Se transporters in terms of their biofortification and phytoremediation implications. Figure 1.1 presents a visual synthesis of the known mechanisms of Se transport in a conceptual map.

1.3.1 Selenium Uptake at the Root

There are four groups of sulfate transporters in plants, all of which are H^+/sulfate symporters (Gigolashvili and Kopriva, 2014). Group 1 SULTRs 1;1, 1;2, and 1;3 are high affinity transporters. SULTR1;1 and SULTR1;2 function to take up sulfate at the root (Yoshimoto et al., 2002), and studies in model species *Arabidopsis thaliana* have shown that both SULTRs are capable of transporting selenate as well. SULTR1;2 is the primary selenate and sulfate transporter, and SULTR1;1 takes up both ions to a significant but lesser extent (Barberon et al., 2008).

The expression levels of SULTR1;1 and SULTR1;2 are partially determined by the concentration of sulfate available at the roots. SULTR1;2 mRNA is approximately 10 times more highly expressed than SULTR1;1 under normal S conditions (Rouached et al., 2008). Both SULTR genes are more highly expressed under S deficiency conditions, although the increase in

SULTR1;1 relative to control conditions is greater than that of SULTR1;2 (Rouached et al., 2008; Yoshimoto et al., 2002). Theoretically, increased expression of both SULTRs may also be expected when selenate is added to the substrate, because selenate competes with sulfate for binding to the SULTRs, effectively mimicking S starvation (Takahashi et al., 2000; Van Hoewyk et al., 2008). However, studies report conflicting results regarding SULTR1;1 and SULTR1;2 upregulation in *A. thaliana* plants exposed to selenate (Rouached et al., 2008; Takahashi et al., 2000; Zhang et al., 2006). The effect of selenate competition with sulfate thus remains unclear. Overall, SULTR1;1 and SULTR1;2 have somewhat overlapping functions, and the nature of their relationship and regulation is still undetermined. However, there is general agreement that SULTR1;2 is the predominant root sulfate and selenate uptake protein.

Although there is less research on the uptake of selenite at the root, recent studies in rice (*Oryza sativa*) and tobacco (*Nicotiana tabacum*) point to the involvement of inorganic phosphate (Pi) transporters (Song et al., 2017; Zhang et al., 2014). In both studies, overexpression of specific Pi transporters led to significantly greater selenite uptake from the substrate. There is also evidence that the aquaporin NIP2;1 is able to take up selenite in rice (Zhao et al., 2010). These mechanisms are both deserving of further study because selenite is the prevalent form of Se available to plants, like rice, that are generally grown in anoxic soils (paddies). Understanding how plants take up selenite from anoxic soils will be useful for the engineering of crops in regions where dietary Se is limited.

Organic Se compounds, including selenoamino acids, can make up a significant proportion of the available soil Se in some soils (Abrams et al., 1990; El Mehdawi et al., 2015a). Plants are able to take up the amino acids selenocysteine (SeCys) and selenomethionine (SeMet) from the soil (Kikkert and Berkelaar, 2013), probably via root amino acid transporters with

affinity for the S analogs cysteine (Cys) and methionine (Met). *A. thaliana* amino acid permease AAP1 and the AAP homolog LHT1 are broad-specificity amino acid transporters that have been shown to mediate uptake of Cys and Met (Boorer et al., 1996; Hirner et al., 2006). More research is required to experimentally determine whether these transporters take up selenoamino acids in addition to their S homologs.

1.3.2 Selenium Translocation Through the Plant

1.3.2.1 Movement between Organs

Several studies in wheat (*Triticum aestivum*) and rice indicate that, following uptake at the root, most selenate is translocated to the shoot (Huang et al., 2017; Li et al., 2008; Wang et al., 2015). It should be noted that similar studies of selenate distribution have not yet been performed in *A. thaliana*, but it is assumed here that the findings of such studies would be analogous to those in rice and wheat.

The low-affinity Group 2 SULTR2;1 and Group 3 SULTR3;5 are expressed in the xylem parenchyma and pericycle in *A. thaliana* and cooperate to load sulfate to the xylem (Kataoka et al., 2004a; Takahashi et al., 2000). SULTR2;1 appears to be the major transporter—while loss of SULTR3;5 somewhat reduces sulfate transport, loss of SULTR2;1 causes a much greater reduction of transport capacity (Kataoka et al., 2004a). Similar to the Group 1 SULTRs, SULTR2;1 expression appears to be inducible under S starvation conditions (El Mehdawi et al., 2018; Shinmachi et al., 2010) or when Se in the substrate is high (Takahashi et al., 2000). Conversely, SULTR3;5 expression is largely unaffected by S level (Kataoka et al., 2004a). Although there is no direct evidence, their functional similarity to the Group 1 SULTRs indicates that SULTR2;1 and SULTR3;5 are likely capable of transporting selenate as well.

Less is known about the redistribution of selenate and sulfate through the phloem. One early study indicated that high-affinity SULTR1;3 localizes to phloem companion cells in both roots and shoot, and plays a role in the mobilization of sulfate to sink organs (Yoshimoto et al., 2003). More recently, SULTR1;3 expression was shown to be upregulated in response to selenate treatment in wheat (Boldrin et al., 2016). Further studies are needed to elucidate the precise function of this transporter.

1.3.2.2 Intracellular Movement

In the vacuole, Group 4 SULTR4;1 and SULTR4;2 both mediate sulfate efflux (Kataoka et al., 2004b). Transcription analyses in *A. thaliana* found that both SULTRs are more highly expressed in the shoot and are upregulated in response to high Se in the substrate (Zhang et al., 2006). This may be because competition with Se simulates S starvation, triggering export of stored sulfate from the vacuole to maintain S status. This would likely release stored selenate from the vacuole as well.

There are no known vacuolar sulfate importers. However, there are several pieces of evidence that together suggest a mechanism for influx of sulfate and selenate via anion channels. First, because the vacuolar lumen is positively charged relative to the cytosol (Martinoia et al., 2000), it is feasible that anions like selenate and sulfate could move passively into the vacuole down their electrochemical gradients via anion channels. Importantly, two parallel studies reported the discovery of channel-like transport proteins that mediate Pi influx to the vacuole (Liu et al., 2015, Liu et al., 2016). A much earlier study showed that Pi uptake into the vacuole was inhibited by competition with chromate, a sulfate analog (Massonneau et al., 2000). This indicates that sulfate (and thereby selenate) could move into the vacuole through these Pi transporters.

Sulfate uptake to the chloroplast is mediated by the five Group 3 SULTRs (3;1-3;5). Interestingly, chloroplast import constitutes a second distinct function for SULTR3;5, in addition to xylem loading (as discussed in Section 2.2.1). Studies of *A. thaliana* Group 3 SULTR mutants found that each of these SULTRs partially contributed to sulfate uptake (Cao et al., 2013; Chen et al., 2019). Interestingly, knockouts of any one of the SULTRs 3;2, 3;3, or 3;4 demonstrated approximately 70% reduced sulfate uptake to the chloroplast. Knockouts of the other two SULTRs (3;1 and 3;5) caused significantly less sulfate uptake reduction. Regarding the overlapping contributions of the Group 3 SULTRs to sulfate uptake (especially 3;2, 3;3 and 3;4), the authors speculate that multiple different SULTRs may complex into a multimer, the function of which is lost or greatly reduced by the loss of any one subunit (Cao et al., 2013). This suggestion has not been experimentally supported. Regardless of the specific mechanism, it is likely that sulfate and selenate are taken up into the chloroplast by the Group 3 SULTRs.

There are no known chloroplast sulfate exporters. It is possible that selenate and sulfate move passively out of the chloroplast down their electrochemical gradients, because the overall charge in the chloroplast stroma is more negative than the cytosol (Pottosin and Shabala, 2016). However, to our knowledge, research into the existence of an anion channel or other transporter to export sulfate from the chloroplast has not been conducted to date. This may be because sulfate is assimilated into the S metabolic pathway in the chloroplast. Thus, mechanisms for export of S-containing metabolites, like the amino acids Cys and Met or the antioxidant glutathione (GSH), may be more physiologically relevant (Gigolashvili and Kopriva, 2014).

1.3.3 Biofortification and Phytoremediation Implications

The primary goal shared by Se biofortification and phytoremediation is to increase Se uptake from the soil. Without this foundation, subsequent goals such as improving plant Se

tolerance or developing tissue-specific accumulation of selenoamino acids cannot be fully realized. Therefore, research to biofortify crops with Se or to remediate Se-rich soils should first focus on increasing Se uptake at the root. As discussed in Section 1.3.1, studies have already shown that both SULTR1;1 and SULTR1;2 are capable of transporting selenate in addition to sulfate. However, there has been little research into the effect of overexpression of these SULTRs on Se accumulation in crop species. A 2016 study demonstrated that tobacco plants overexpressing the soybean (*Glycine max*) SULTR1;2 homolog exhibited increased biomass and S content (Ding et al., 2016)—however, Se content of the transgenics and control plants were not reported. Similar studies could also analyze the effects on Se accumulation of overexpressing phosphate transporters, aquaporins like NIP2, and amino acid transporters. To our knowledge, no such studies have yet been performed.

1.4 Selenium Metabolism, Toxicity, and Tolerance

Similarly to Se transport, Se metabolism in plants is predicted to largely follow the S pathway (White, 2018). However, there is significantly more experimental evidence to support this assertion for Se metabolism than for Se transport. Section 1.4.1 proceeds stepwise through the S assimilation pathway, discussing evidence indicating that Se assimilation follows the same route. Major branch points in the pathway are noted. Section 1.4.2 describes the specific mechanisms of Se toxicity, and Section 1.4.3 reviews the major methods of Se tolerance. Finally, Section 1.4.4 discusses significant questions of biofortification and phytoremediation which can be addressed by this research. Figure 1.2 diagrams the known steps of the S and Se metabolic pathways.

1.4.1 Selenium Metabolism

1.4.1.1 From Selenate to Selenocysteine

Although Se and S assimilation may occur in the root or shoot, most selenate taken up by the plant is transported to the shoot (Leustek, 1996; Pilon-Smits et al., 1999; Sors et al., 2005b). The S and Se assimilation pathways then split into cytosolic and plastidic branches. In the former, sulfate is activated to adenosine 5'-phosphosulfate (APS) by the cytosolic isoform of the enzyme adenosine triphosphate sulfurylase (ATPS2) (Bick and Leustek, 1998; Bohrer et al., 2015b). Studies of yeast ATPS have shown that it acts on sulfate and also assimilates selenate to adenosine 5'-phosphoselenate (APSe) (Dilworth and Bandurski, 1977; Raspor et al., 2003). Furthermore, overexpression of ATPS1 in the plant species *Brassica juncea* and *A. thaliana* increased selenate reduction to APSe (Pilon-Smits et al., 1999; Sors et al., 2005a). In the next step, APS is phosphorylated to 3′-phosphoadenosine 5′-phosphosulfate (PAPS) by APS kinase (APK) (Bohrer et al., 2015a). PAPS serves as a donor of S for sulfated metabolites (Koprivova and Kopriva, 2016). It is not known whether APK also acts on APSe. More research is required to determine the fate of Se in the cytosol in plant shoots.

Significantly more research has been conducted to elucidate the plastidic branch of the S and Se assimilation pathways. Selenate, by analogy with sulfate, is probably able to enter the chloroplast of leaf cells via the Group 3 SULTRs (Chen et al., 2019). In the chloroplast, sulfate and selenate are reduced to cysteine (Cys) and selenocysteine (SeCys), respectively (Sors et al., 2005b; White, 2018).

The first enzyme of this pathway is also ATPS, which has 4 plastidic isoforms. In *A. thaliana*, ATPS1, ATPS3 and ATPS4 localize only to the chloroplast, and ATPS2 is found in both the chloroplast and cytosol (Bohrer et al., 2015a, 2015b). In the plastid, ATPS activates

sulfate and selenate to APS and APSe, respectively. Next, APS reductase reduces APS to sulfite (Setya et al., 1996). Evidence indicates that this enzyme likely also acts to reduce APSe to selenite: a study of transgenic *A. thaliana* showed that overexpressing ATPS or APS reductase each increased the proportion of selenite in the plant, but that overexpressing both increased reduction to selenite still more highly (Sors et al., 2005a). This suggests that both enzymes work together, not only to reduce sulfate, but also selenate.

Sulfite and selenite are then further reduced to sulfide and selenide, respectively. The reduction of sulfite is performed by the enzyme sulfite reductase (SiR). However, it is not clear whether this enzyme is also capable of reducing selenite. Multiple studies have shown that inhibition or knockdown of SiR do not affect selenite reduction to selenide (Fisher et al., 2016; Ng and Anderson, 1979). It appears that reduction of selenite via an interaction with glutathione is more energetically favored (Hsieh and Ganther, 1975).

The Cysteine Synthase (CS) complex, established via a reversible complexation of O-acetylserine thiol lyase (OASTL) and serine acetyltransferase (SAT), incorporates sulfide into Cys (Bogdanova and Hell, 1997). This complex can be found in the mitochondria and cytosol in addition to the chloroplast (Heeg et al., 2008). *In vitro* studies of this complex isolated from several plant species have confirmed that it is also capable of incorporating selenide into SeCys (Ng and Anderson, 1978). There are two major branches in the S/Se metabolic pathway following production of Cys/SeCys. The first releases elemental Se from SeCys, and the second is the production of selenomethionine (SeMet), another selenoamino acid (Lima et al., 2018; White, 2018).

1.4.1.2 Release of Elemental Selenium from Selenocysteine

Research in *A. thaliana* revealed that the chloroplast-localized cysteine desulfurase AtCpNifS is capable of both releasing elemental S from Cys and elemental Se from SeCys. Activity assays demonstrated that the enzyme more efficiently reacts with SeCys than Cys (Pilon-Smits et al., 2002). Elemental S released by AtCpNifS in the chloroplast may be used in the subsequent formation of Fe-S clusters, important cofactors for proteins involved in the photosynthetic electron transport chain (Balk and Lobréaux, 2005). It is possible that Se is subsequently misincorporated into Fe-Se clusters, damaging the photosynthetic apparatus. Interestingly, however, *A. thaliana* overexpressing AtCpNifS demonstrated overall increased tolerance to selenate, possibly due to reduced concentrations of SeCys (Van Hoewyk et al., 2005).

1.4.1.3 From Selenocysteine to Selenomethionine

In vitro studies of the enzyme cystathionine-gamma-synthase (CγS) from spinach (*Spinacia oleracea*) extract demonstrated that it is capable of synthesizing cystathionine (CysTH) as well as selenocystathionine (SeCysTH), from Cys and SeCys, respectively (Dawson and Anderson, 1988). Subsequently, CysTH and SeCysTH are split to form homocysteine (HCys) and selenohomocysteine (SeHCys), respectively, by cystathionine-beta-lyase (CβL). This step was again confirmed by *in vitro* analysis of crude plant extracts, including spinach extract (McCluskey et al., 1986).

Methionine synthase (MetH) catalyzes the final step of Met synthesis from HCys in plants. No experiments have yet shown that plant MetH is also capable of synthesizing selenomethionine (SeMet) from SeHCys. However, mammalian MetH has been used to catalyze SeMet synthesis (Zhou et al., 2000). Both SeMet and SeCys have long been known to

accumulate in plants following Se treatment (Peterson and Butler, 1962). Therefore, it is most likely that plant MetH acts upon SeHCys as well. Up to this point, all steps of the Se metabolic pathway have occurred within the chloroplast. However, the localization of the final step in SeMet synthesis is unclear. Studies in *A. thaliana* have shown that MetH isoforms exist both in the cytosol (Ravanel et al., 1998) and the chloroplast (Ravanel et al., 2004).

1.4.1.4 Volatile Product from Selenomethionine

From Met and SeMet, plants can synthesize the volatile compounds dimethylsulfide (DMS) and dimethylselenide (DMSe), respectively. First, the enzyme S-adenosyl-L-Methionine:L-Methionine S-methyltransferase (MMT) methylates SeMet to Se-methyl selenomethionine (SeMM) (Tagmount et al., 2002). DMSe is then released from SeMM in one of two ways. In some plants, the enzyme methylmethionine hydrolase (MMH) cleaves SeMM and releases volatile DMSe directly (Lewis and Johnson, 1974). Alternatively, in other species SeMM may be converted to the intermediate dimethylselenonium propionate (DMSeP) (Tagmount et al., 2002). While there is no direct evidence for this, *B. juncea* plants supplied with DMSeP volatilized Se (as DMSe) at a rate six times that of plants supplied with SeMet (De Souza et al., 2000). This indicates that DMSeP is likely an intermediate that is quickly converted to volatile DMSe, via an unknown process.

1.4.2 Toxic Selenocompounds and their Effects

1.4.2.1 Selenocysteine and Selenomethionine

Overall Se toxicity, as measured by reduction in dry weight productivity, is correlated to the ratio of Se to S concentrations in the shoot (White et al., 2004). This suggests that a major mechanism of Se toxicity is competition with S. This competition mainly manifests as the misincorporation of SeCys and SeMet in place of Cys and Met in protein synthesis.

Selenocysteine is thought to be the major source of problematic misincorporation into proteins (Van Hoewyk, 2013). Cys residues are often found at key locations in tertiary protein structures. For example, SeCys substitution for Cys at an active site can either enhance or inhibit activity at that site. Cys residues are also often found at metal binding sites. SeCys incorporation at such sites can alter the strength of the metal bond. Another major aspect of protein structure is the disulfide bridge, which is the covalent bond between the S atoms of two Cys residues adjacent to each other in the tertiary structure. SeCys substitution at these locations can change the bridge properties and affect overall protein structure and function. Finally, within the NifS-like proteins, SeCys substitution can lead to the production of Fe-Se instead of Fe-S clusters, which can damage critical photosynthetic processes (Van Hoewyk, 2013). For example, *Stanleya albescens* plants demonstrated photosynthetic rate reductions when grown on media with 20μM selenate (Freeman et al., 2010).

SeMet is significantly less deleterious when incorporated into proteins than SeCys. The general toxicity mechanism of SeMet misincorporation stems from the fact that the rate of peptide bond formation between SeMet and subsequent amino acids is reduced relative to Met. Because Met is the amino acid encoded by the initiation codon, this can lead to an overall reduced rate of translation initiation, providing that the concentration of available SeMet is sufficiently high to compete with Met (Eustice et al., 1981; Van Hoewyk, 2013).

1.4.2.2 Selenate and Selenite

Experimental evidence indicates that selenate exposure correlates strongly to increased accumulation of reactive oxygen species (ROS), which cause many types of physiological damage. Exposure to 20μM Se as selenate via the growth media was sufficient to induce excess accumulation of the ROS superoxide and hydrogen peroxide in *S. albescens* plants (Freeman et

al., 2010). A study of the effect of selenate on *A. thaliana* found that knocking out APS reductase, involved in the reduction of selenate to selenite, causes a higher accumulation of ROS than in wild type, in selenate-exposed plants. In APR knockout plants, excess accumulation of selenate was found to correlate to reduced levels of GSH (Grant et al., 2011). This is problematic because it reduces the plant's overall antioxidative capacity.

Selenite may be more toxic to plants than selenate. Multiple studies show that adverse effects of Se begin to appear at lower concentrations of selenite than selenate. In cabbage and cucumber, biomass was found to decrease at lower concentrations of supplied selenite than selenate, and lipid peroxidation (free radical damage to lipids) increased significantly at lower selenite concentrations as well. Se concentrations were also higher in the roots of plants supplied with selenite, and higher in the shoots when supplied with selenate (Hawrylak-Nowak, 2013). All of the same results were also found in a later study of cucumber plants (Hawrylak-Nowak et al., 2015). The prevailing theory regarding the toxicity of selenite is that, whereas selenate is transported to the shoot and mostly remains as selenate, selenite is largely assimilated in the root into organic Se compounds like SeCys and SeMet, interfering with normal protein production (White, 2018).

1.4.3 Mechanisms of Selenium Tolerance

Plants tolerate Se via a combination of several mechanisms. The major tolerance mechanisms appear to be GSH intervention and volatilization of DMSe. GSH has been reported to interact with selenate. This interaction produces oxidized GSH and reduces the level of selenate (Grant et al., 2011), which prevents some selenate from creating ROS, but also reduces overall levels of available GSH in the plant. Volatilization of DMSe also has been shown to significantly reduce the Se load of the plant (Lewis and Johnson, 1974).

Other mechanisms only moderately reduce Se toxicity, or only theoretically affect tolerance. For example, *A. thaliana* expresses proteins homologous to the mammalian Se-binding proteins, and these may be involved in increasing Se tolerance (Agalou et al., 2005). However, the significance of this effect has not been studied. In addition, the action of AtCpNifS can release elemental Se from SeCys, and overexpression of AtCpNifS has been shown to increase Se tolerance (Van Hoewyk et al., 2005). While elemental Se is not toxic in itself, it may be misincorporated into Fe-Se clusters, so the net effect of this mechanism at higher levels of Se is unknown. Finally, a significant proportion of selenate is stored in the vacuoles of leaf cells—this selenate may be remobilized via the vacuolar S transport proteins SULTR4;1 and SULTR4;2 (Zhang et al., 2006).

1.4.4 Biofortification and Phytoremediation Implications

Overexpression of key enzymes in the Se metabolic pathway may improve plant species' ability to accumulate larger quantities of Se without suffering toxic effects. Several enzymes have already been tested. Studies have demonstrated that both ATPS and APR are good candidates for overexpression to enhance reductive selenate assimilation. ATPS1 from *A. thaliana* overexpressed in *B. juncea* led to increased Se uptake and a greater proportion of Se reduced to nontoxic organic forms (Pilon-Smits et al., 1999). A later study of *A. thaliana* showed that plants overexpressing either endogenous ATPS1 or APR from the bacterium *Pseudomonas aeruginosa* reduced proportionally more selenate than control plants, and that plants constitutively expressing both enzymes were able to reduce still more (over 90%) selenate (Sors et al., 2005a). Furthermore, plants overexpressing ATPS1 had increased GSH levels (Pilon-Smits et al., 1999; Sors et al., 2005a), which should help the plant maintain proper redox status, and also may be involved in the reduction of APSe to selenite (Dilworth and Bandurski, 1977). In

field trials, a *B. juncea* transgenic line overexpressing *A. thaliana* ATPS1 was also found to accumulate over four times more Se than the wild type when grown on Se-contaminated soils (Bañuelos et al., 2005).

The next enzyme in the pathway to SeCys synthesis is the Cysteine Synthase complex. The effect of overexpressing this complex on Se toxicity in plants has not yet been examined. Overexpression of the complex has been shown to increase Cys production and tolerance to toxic S-containing compounds in tobacco—however, the tolerance to Se has not been tested (Noji et al., 2001). Since Cys production was increased, toxic SeCys production would likely be increased as well. However, this could merit experimental analysis, especially if CpNifS is concurrently overexpressed. As mentioned in Section 1.4.1.2, AtCpNifS catalyzes the release of elemental Se from SeCys at a much higher rate than S from Cys (Pilon-Smits et al., 2002; Van Hoewyk et al., 2005). Furthermore, although Se could be subsequently misincorporated into Fe-Se complexes, there is no evidence yet that this occurs to a sufficient extent that it has negative consequences for the plant (Van Hoewyk et al., 2005).

Enzymes involved in the production of SeMet from SeCys are also promising, because Se accumulated as SeMet is less toxic than SeCys (Van Hoewyk, 2013). The first enzyme in this pathway, cystathionine-gamma-synthase (CγS), has been tested. Transgenic *B. juncea* expressing *A. thaliana* CγS demonstrated increased volatilization of DMSe and increased tolerance to selenite, but not selenate (Van Huysen et al., 2003). Several species expressing *A. thaliana* CγS have also been shown to accumulate increased levels of Met (Amir, 2010). Overexpression of the next enzyme in the pathway, cystathionine-beta-lyase, has been shown to not significantly increase the amount of Met accumulated in potato (*Solanum tuberosum*) (Maimann et al., 2001). The final enzyme, methionine synthase (MetH), has not been tested. Nevertheless, the increase in

Met accumulation and DMSe volatilization in plants overexpressing CγS indicates that this enzyme is more likely to be rate-limiting than CβL or MetH. CγS warrants further testing in other species of interest for phytoremediation.

It is unclear whether overexpressing enzymes involved in the synthesis of DMSe from SeMet increases the volatilization of Se. This is partly because research on these enzymes is limited to date. Overexpression in *Escherichia coli* of the first enzyme in this pathway, S-adenosyl-L-Methionine:L-Methionine S-methyltransferase (MMT), increased the volatilization of DMSe tenfold compared to an untransformed control (Tagmount et al., 2002), but to our knowledge no similar study has been done in plants. Furthermore, no study has assessed the effect of overexpressing the subsequent enzyme, methylmethionine hydrolase. In some plants, it appears that the compound DMSeP is an intermediate between SeMM and DMSe. It has been shown that the production of DMSeP from SeMet is rate-limiting for Se volatilization, rather than the production of DMSe from DMSeP (De Souza et al., 2000). However, the enzymes involved in both of these steps are still unknown and must be discovered before transgenic experiments can be performed.

1.5 Selenium Hyperaccumulators

Many plant species experience reduced fitness when grown on soils with high concentrations of Se (Freeman et al., 2010; Mikkelsen et al., 1989; Xue et al., 2001). However, some species have adapted to not only tolerate but thrive on high concentrations of Se. These species, called Se hyperaccumulators (HAs), preferentially take up Se from the soil and accumulate it to tissue concentrations reaching 1.5% of their dry weight, which is hundreds of times higher than adjacent vegetation (Cappa et al., 2014). This capability benefits plant fitness in several ways. At low levels, Se accumulation improves antioxidant capacity, possibly by

stimulating expression of stress response genes (Freeman et al., 2010). At higher levels, ecological benefits emerge, including herbivore deterrence and toxicity (El Mehdawi et al., 2015b; Galeas et al., 2008) and elemental allelopathy for surrounding vegetation (Schiavon and Pilon-Smits, 2017). These species possess unique adaptations which allow for the accumulation and tolerance of such extreme levels of Se. Section 1.5.1 discusses the current state of knowledge regarding Se uptake and transport in HAs. Section 1.5.2 describes the differences between HA Se metabolism and normal Se metabolism, noting HA-specific mechanisms of Se tolerance. Section 1.5.3 briefly reviews other HA adaptations, including ecological benefits and plant stress response adaptations. Section 1.5.4 analyzes the potential applications of Se HAs for biofortification and phytoremediation. Figure 1.2 includes metabolic processes unique to HAs.

1.5.1 Uptake and Transport

Several lines of evidence indicate that Se HAs possess mechanisms to preferentially take up Se over S, or to translocate Se preferentially over S to shoot tissues. A study of 39 angiosperm species, comprising HA and non-HA species, found a larger Se:S ratio in the leaves of HAs (P. J. White et al., 2007). Leaf Se concentration was significantly higher in the HAs; sulfur levels were also higher in the HAs but not as elevated as Se. Another study, comparing HA *Stanleya pinnata* and related non-HA *B. juncea*, found that uptake of selenate was significantly less inhibited by the presence of competing sulfate for the HA than the non-HA, suggesting that the HA has at least one selenate-specific transporter (Harris et al., 2014). The underlying mechanism is uncertain, but a number of transporters may be involved in this process.

Recent transcriptomic analyses indicate that hyperaccumulators may regulate the expression of SULTRs differently than related non-HAs. For example, the HA *S. pinnata* has been demonstrated to constitutively upregulate several SULTRs, whereas non-HA sister species

S. elata regulates these SULTRs with respect to the concentrations of supplied sulfate and selenate (Wang et al., 2018). Specifically, the HA constitutively expresses the root uptake protein SULTR1;2, root to shoot translocator SULTR2;1, phloem transporter SULTR1;3 (in the root only), chloroplast importer SULTR3;1 (in the shoot only), and vacuolar exporter SULTR4;1 (in the root only) (Wang et al., 2018). Another possible candidate for preferential root uptake is the amino acid transporter LHT1, which was hundreds of times more highly expressed in the roots of *S. pinnata* than *S. elata* (Wang et al., 2018). As discussed in Section 2.1, LHT1 is a broad-specificity amino acid transporter capable of taking up of Cys and Met (and therefore possibly SeCys and SeMet) in plant roots (Hirner et al., 2006).

The form of supplied Se may also have a significant effect on the response of a HA. A recent transcriptomic analysis of the Se HA *Cardamine hupingshanensis* found that, when supplied with selenite, the HA in fact downregulated the expression of its SULTR1;2 homolog (Zhou et al., 2018). This result may be attributable to the fact that selenite is not likely to be transported through SULTRs, but rather through Pi transporters, due to the greater similarity of Pi to selenite (White, 2018). Interestingly, a recent study of the related HA *C. violifolia* found that supplied phosphate did not interfere with selenite uptake (Both et al., 2020), indicating that selenite might instead be taken up via aquaporins, as has been shown in rice with the aquaporin NIP2;1 (Zhao et al., 2010).

Hyperaccumulation is thought to have evolved independently many times (Cappa and Pilon-Smits, 2014); thus, different taxa may have evolved different and perhaps unique methods of Se accumulation. The best-studied HA so far are *Astragalus bisulcatus* (Fabaceae) and *Stanleya pinnata* (Brassicaceae). In a transcriptomic analysis of multiple Se HA and non-HA species from the genus *Astragalus*, SULTR transcripts were generally found to be constitutively

expressed across all species, regardless of supplied selenate or sulfate concentration (Cabannes et al., 2011). This was a surprising result, as previously the constitutive upregulation of various SULTRs had been considered a hallmark of Se hyperaccumulators.

SULTR1;2 is the only transporter, to our knowledge, that has been isolated and tested for sulfate and selenate transport affinities. SULTR1;2 homologs from the HA *S. pinnata* and non-HA *S. elata* were expressed in yeast, and overall Se and S accumulation in transformed yeast supplied with several concentrations of selenate and sulfate were compared. Overall, no conclusive evidence was found to support the contention that the HA SULTR1;2 had a greater specificity for selenate over sulfate, when compared to the non-HA SULTR1;2 (Guignardi, 2017). Similar studies should be undertaken to determine which, if any, SULTRs or other transport proteins demonstrate Se specificity in hyperaccumulator species.

1.5.2 Metabolism and Tolerance

Hyperaccumulator and non-HA metabolism of Se differ in several ways, beginning at the first step, the reduction of selenate. Non-accumulators can reduce selenate via any of four ATPS isoforms (ATPS1-4). ATPS1, 3, and 4 localize to the plastid, and ATPS2 localizes to both the plastid and cytosol. The HA *S. pinnata*, on the other hand, expresses ATPS2 in the root 10 times higher than the other three isoforms (Wang et al., 2018). Furthermore, in this HA, ATPS2 only localizes to the cytosol (Jiang et al., 2018). In most plants, the majority of selenate is moved directly from the roots to the shoots—however, high concentrations of both ATPS2 transcripts and selenoamino acids have been found in *S. pinnata* roots, and ATPS2 expression is especially high in low-S conditions, with or without the presence of competing Se (Schiavon and Pilon-Smits, 2017).

Some SeCys in HAs may be methylated to methylselenocysteine (MeSeCys) by the action of selenocysteine methyltransferase (SMT). Accumulation of this amino acid is not correlated to Se toxicity symptoms because it cannot be incorporated in place of Cys in polypeptides—thus, it does not interfere with normal protein synthesis (Neuhierl and Böck, 1996). SMT was first discovered in the hyperaccumulator *Astragalus bisulcatus* (Neuhierl and Böck, 1996). However, subsequent research indicates it is present in at least some non-HA species as well (Bañuelos et al., 2007; Lyi et al., 2005). Overexpression of the *A. bisulcatus* SMT in *A. thaliana* led to several HA-like phenotypes: higher proportion of Se as MeSeCys, higher Se tolerance, higher Se accumulation overall, and greater volatilization of Se (LeDuc et al., 2004). Furthermore, in a study of several *Astragalus* species, SMT activity was on average six times higher in the HA species than the non-accumulator species (Sors et al., 2005a). Hyperaccumulator *S. pinnata* also mainly accumulates Se as MeSeCys (Freeman et al., 2006).

Finally, in addition to volatilizing Se as DMSe, hyperaccumulators are capable of volatilizing Se as dimethyldiselenide, DMDSe. This volatile compound is produced from MeSeCys. First, MeSeCys may be converted to the methylselenocysteine selenoxide (MeSeCysSeO) intermediate (Arnold and Thompson, 1962) via an as-yet uncharacterized enzyme, or it may be converted directly to methaneselenol (MSe) by cysteine sulfoxide lyase (CSL) (Hall and Smith, 1983). MSe is subsequently converted to DMDSe (Gabel-Jensen et al., 2010; Ranjard et al., 2002).

1.5.3 Other Hyperaccumulator Adaptations

The ability to accumulate high concentrations of Se confers a number of plant health benefits to Se HAs. Strong evidence indicates that Se HAs gain an ecological advantage in herbivore deterrence, without apparent deterrence of important pollinator species. HAs tend to

concentrate Se in their epidermis (Freeman et al., 2006), which both sequesters it away from S metabolic processes and deters biotic attackers. There is also evidence that soil Se phytoenrichment from hyperaccumulator leaf litter acts as a form of elemental allelopathy by deterring the growth of Se-sensitive vegetation close to hyperaccumulator plants. These ecological adaptations have been reviewed extensively elsewhere (El Mehdawi and Pilon-Smits, 2012; Schiavon and Pilon-Smits, 2017).

Selenium HA species also appear to possess heightened stress response mechanisms as compared to normal plants. The stress defense hormones ethylene, jasmonic acid, and salicylic acid—which upregulate antioxidant mechanisms and biotic stress resistance processes—are constitutively expressed in the HA *S. pinnata* (Freeman et al., 2010; Wang et al., 2018). Overproduction of any of these hormones may also increase S and Se uptake and assimilation in hyperaccumulators (Wang et al., 2018). Several studies in non-HA species support the idea that upregulation of these defense hormones can provide protection from Se stress. For example, Se-resistant accessions of the non-HA *A. thaliana* were found to upregulate stress defense hormones in response to Se exposure (Tamaoki et al., 2008). In another study, *B. juncea* plants treated with toxic concentrations of Se demonstrated greater growth inhibition than plants treated with both Se and salicylic acid (Gupta and Gupta, 2016). Finally, a recent study found that overexpression of the ethylene response factor ERF96 in *A. thaliana* increases selenite resistance, through both increased antioxidative capacity and reduced Se uptake (Jiang et al., 2020).

1.5.4 Biofortification and Phytoremediation Implications

The current understanding of Se transport in hyperaccumulators remains limited. It is clear that HAs regulate some Se transport proteins differently than non-HAs, and overexpress certain SULTR proteins, which may explain their high Se accumulation. However, no study has

yet explained the high Se:S ratios characteristic of Se HAs. Therefore, Se HA transporters will benefit from significant further study before they are applied to biofortification or phytoremediation. In particular, identification of a selenate-specific transporter would be very beneficial for the creation of transgenics that can effectively take up Se in a high-S environment.

There are several HA enzymes involved in reductive Se metabolism that may also be overexpressed in species of interest for biofortification and phytoremediation. Hyperaccumulator *S. pinnata* appears to rely disproportionately on the isoform ATPS2 for selenate reduction to APSe (Jiang et al., 2018). This isoform should be tested in comparison to the primary isoforms used by non-HA species to determine whether HA ATPS2 can reduce selenate more effectively or has other unique properties.

Other promising enzymes for the improvement of phytoremediation and biofortification capabilities are those involved in the synthesis of MeSeCys and subsequent volatilization of DMDSe. In some species, MeSeCys can be converted to methaneselenol by CSL (Hall and Smith, 1983). Then, methaneselenol may be converted to DMDSe by an unknown enzyme. If the rate-limited enzyme in this pathway were identified, it could be overexpressed in non-HA species, and Se volatilization could proceed via two routes (DMSe and DMDSe)—which would significantly improve the capability of phytoremediation practices.

Though it is not the main focus of this review, it should be noted that overexpression of stress response-related genes is also a promising tool for Se biofortification and phytoremediation. Overexpression of genes that increase production of ethylene, jasmonic acid, or salicylic acid has been linked to increased Se tolerance in *A. thaliana* (Tamaoki et al., 2008). Improving Se tolerance is an important factor in the development of plant lines for phytoremediation or biofortification; however, there are potential drawbacks of using stress

hormones to achieve this goal. For example, although increased ethylene production has been shown to improve Se tolerance via increased antioxidative capacity, it can also repress the production of Se transport proteins and ultimately reduce overall Se uptake (Jiang et al., 2020).

1.6 Conclusion

Improvements to Se phytoremediation and crop biofortification require a thorough knowledge of the processes of Se transport and metabolism in plants. Significant in this respect, however, is the fact that plants do not seem to require Se and thus do not have Se-specific pathways. Rather, Se is transported through the action of S transport proteins and metabolized via S metabolic enzymes. Therefore, understanding Se transport and metabolism in plants means understanding the analogous S plant processes. This knowledge can then be applied to enhance Se uptake and assimilation to nontoxic forms in species of interest for Se phytoremediation or biofortification.

Enhancing Se uptake is likely achievable via overexpression of one or more SULTR proteins; this would be particularly effective if any of the HA SULTRs were found to have enhanced selenate-to-sulfate specificity. However, few experiments have been performed in this area to date. Comparatively more research has been conducted into the effects of overexpressing enzymes of the S metabolic pathway on Se accumulation. Transgenic plants overexpressing ATPS, SMT, and CpNifS have been shown to accumulate significantly more Se than wild-type plants. Transgenic *B. juncea* overexpressing the enzyme ATPS grew well (but slowly) on Se-rich soils, and accumulated over four times more Se in their leaves than wild type plants (Bañuelos et al., 2007, 2005).

When developing future studies, it should be noted that the most effective strategies to increase Se accumulation and tolerance will likely combine increased uptake via overexpressed

SULTRs with overexpression of enzymes in the Se metabolic pathway to increase the proportion of nontoxic selenocompounds in the plant. Figure 1.3 suggests two such strategies. Sulfate transporters of interest (in addition to SULTR1;2) include SULTR2;1 and SULTR3;5 (which are likely responsible for root to shoot translocation of selenate), and the Group 3 SULTRs 3;2-3;4 (which are likely the main chloroplast selenate importers). Other enzymes that merit further testing include CpNifS (which releases elemental Se from SeCys), CγS (part of the metabolic pathway from SeCys to SeMet), MMT (part of the metabolic pathway from SeMet to DMSe), and SMT and CSL (part of the metabolic pathway from SeCys to DMDSe). All of these are promising areas for future research.

1.7 Figures

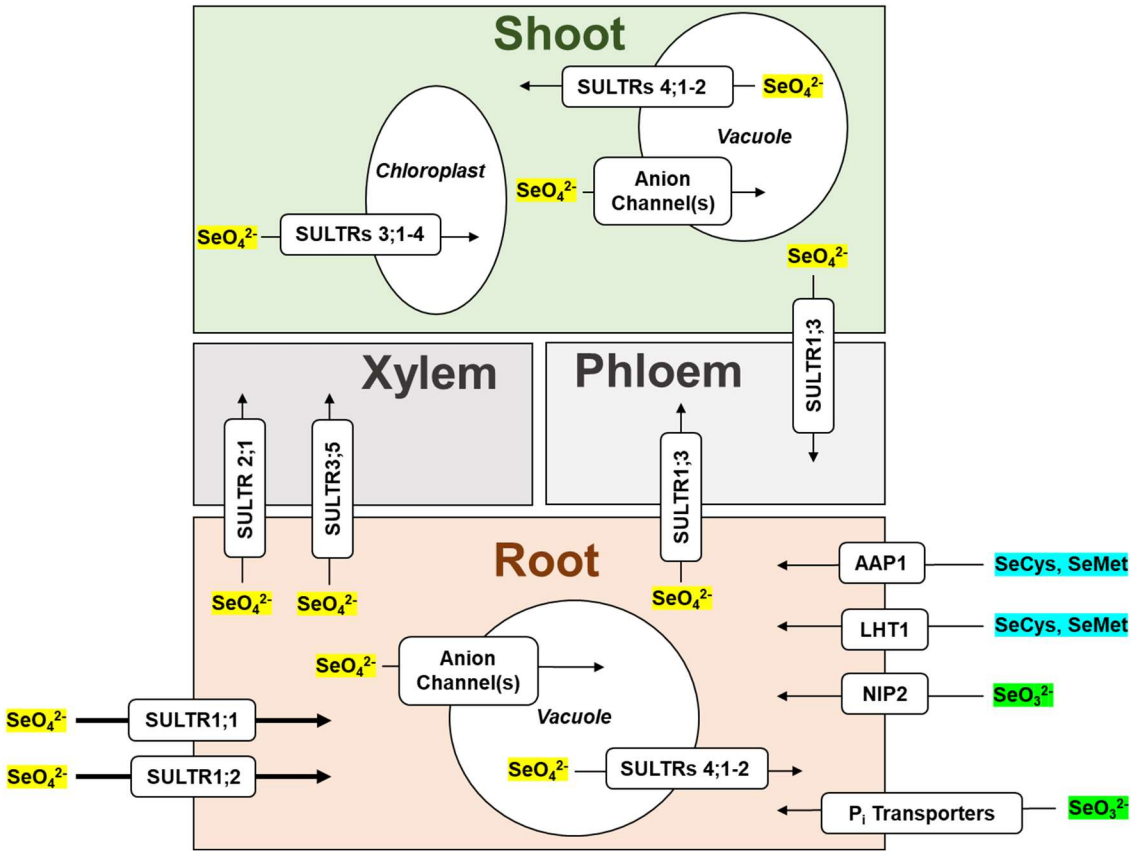

Figure 1.1. Conceptual map of selenium transport in plants. Selenate (SeO_4^{2-}) is highlighted in yellow, selenite (SeO_3^{2-}) is highlighted in green, and the amino acids selenocysteine (SeCys) and selenomethionine (SeMet) are highlighted in blue. Transport of selenate via SULTR1;1 and SULTR1;2 is bolded because there is experimental evidence to support it (Barberon et al., 2008; Takahashi et al., 2000; Van Hoewyk et al., 2008). All other movement of selenocompounds is not bolded because the supporting evidence (discussed in Sections 2.1 and 2.2) is indirect and largely consists of interpretation from transcriptomic analyses.

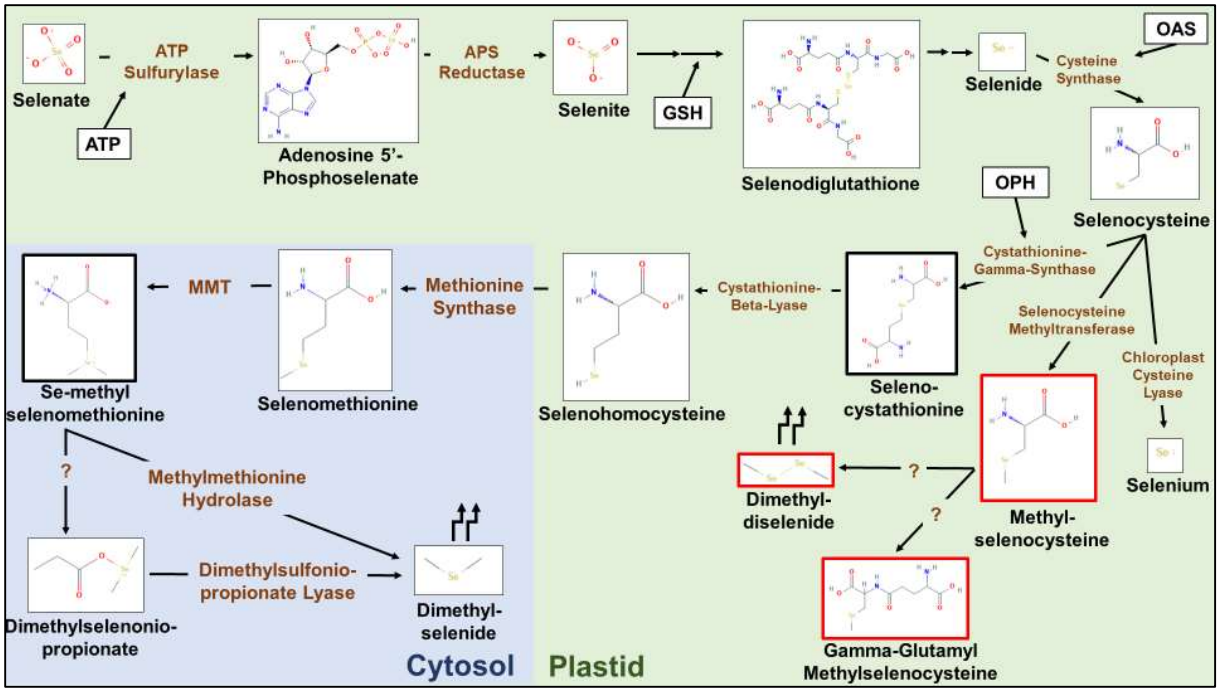

Figure 1.2. Conceptual map of the plastidic pathway of selenium metabolism in plants. The cytosolic pathway (reduction of selenate to adenosine 5'-phosphoselenate by cytosolic ATPS) is not shown here. Plastid-localized reactions on green background; cytosol-localized reactions on blue background. All reactants are shown; for simplicity, only products containing Se are shown. Double arrows indicate steps are not shown. Compounds that are found in high concentrations in Se hyperaccumulators are bordered in bold black. Compounds that are only found in Se hyperaccumulators are bordered in bold red. Kinked double arrows indicate compounds that are volatilized. Several enzymes have alternate localizations not shown here. These include ATP sulfurylase (also found in cytosol) and cysteine synthase (also found in cytosol and mitochondria). ATP: adenosine triphosphate; OPH: O-phosphohomoserine; OAS: O-acetylserine; GSH: glutathione; MMT: S-adenosyl-L-Methionine:L-Methionine S-methyltransferase. All chemical structures obtained from PubChem database (Kim et al., 2019).

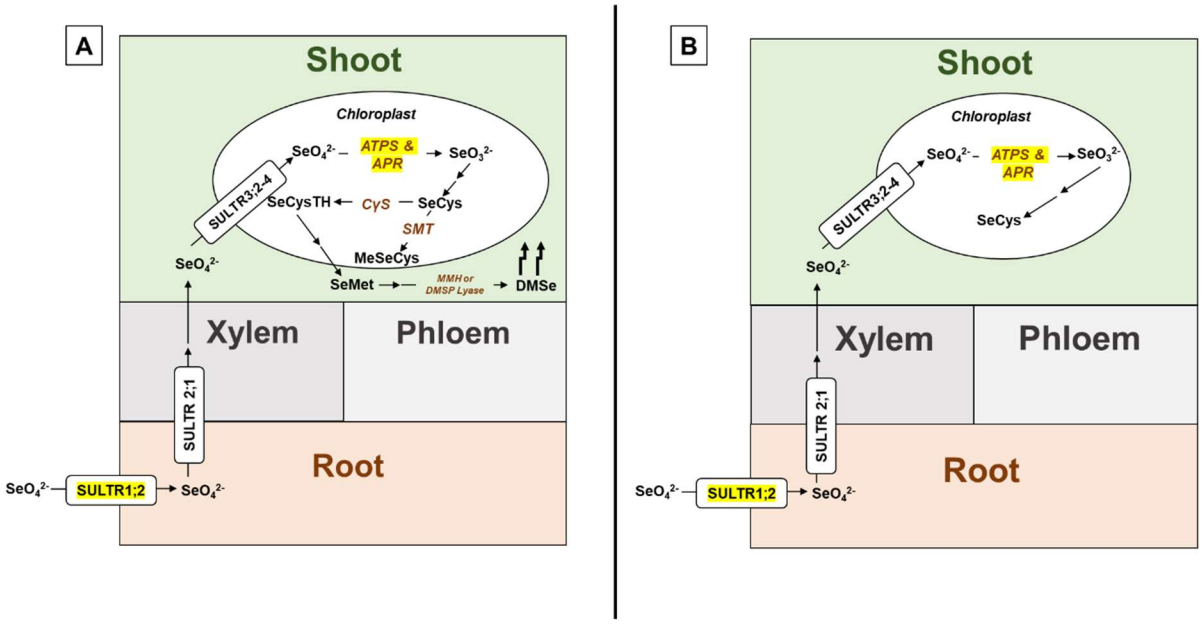

Figure 1.3. Schema for transgenic plants with enhanced Se biofortification or phytoremediation potential. **A.** Generic plant schema with constitutive overexpression of select genes for Se phytoremediation. **B.** Generic crop plant schema with constitutive overexpression of select genes for Se biofortification. Highlighted transporters and enzymes have been experimentally manipulated *in vivo*; other transporters and enzymes have not. Overexpressed SULTRs are in rounded boxes. Overexpressed enzymes are italicized in dark red; selected intermediate selenocompounds are bold in black. Volatilized compounds indicated by kinked double arrows. SeO_4^{2-}: selenate, SeO_3^{2-}: selenite, ATPS: ATP sulfurylase, APR: APS reductase, CγS: cysteine-gamma-synthase, SMT: selenocysteine methyltransferase, SeCys: selenocysteine, MeSeCys: methylselenocysteine, SeCysTH: selenocystathionine, MMH: methylmethionine hydrolase, DMSP: dimethylsulfoniopropionate, DMSe: dimethylselenide.

LITERATURE CITED

Abrams, M.M., Burau, R.G., Zasoski, R.J., 1990. Organic Selenium Distribution in Selected California Soils. Soil Sci. Soc. Am. J. 54, 979–982. https://doi.org/10.2136/sssaj1990.03615995005400040007x

Agalou, A., Roussis, A., Spaink, H.P., 2005. The Arabidopsis selenium-binding protein confers tolerance to toxic levels of selenium. Funct. Plant Biol. 32, 881–890. https://doi.org/10.1071/FP05090

Al-Fageeh, M.B., Smales, C.M., 2006. Control and regulation of the cellular responses to cold shock: The responses in yeast and mammalian systems. Biochem. J. 397, 247–259. https://doi.org/10.1042/BJ20060166

Amir, R., 2010. Current understanding of the factors regulating methionine content in vegetative tissues of higher plants. Amino Acids 39, 917–931. https://doi.org/10.1007/s00726-010-0482-x

Anderson, J.W., 1993. Selenium interactions in sulfur metabolism, in: De Kok, L.J., Stulen, I., Rennenberg, H., Brunold, C., Rauser, W.E. (Eds.), Sulfur Nutrition and Assimilation in Higher Plants: Regulatory Agricultural and Environmental Aspects. SPB Academic Publishing, The Hague, pp. 49–60.

Arnold, W.N., Thompson, J.F., 1962. The formation of (+) S-methyl-L-cysteine sulfoxide from S-methyl-L-cysteine in crucifers. Biochim. Biophys. Acta 57, 604–606.

Arthur, J.R., Nicol, F., Beckett, G.J., 1992. The role of selenium in thyroid hormone metabolism and effects of selenium deficiency on thyroid hormone and iodine metabolism. Biol. Trace Elem. Res. 33, 37–42. https://doi.org/10.1139/y91-243

Balk, J., Lobréaux, S., 2005. Biogenesis of iron-sulfur proteins in plants. Trends Plant Sci. 10, 324–331. https://doi.org/10.1016/j.tplants.2005.05.002

Bañuelos, G., Leduc, D.L., Pilon-Smits, E.A.H., Terry, N., 2007. Transgenic Indian mustard overexpressing selenocysteine lyase or selenocysteine methyltransferase exhibit enhanced potential for selenium phytoremediation under field conditions. Environ. Sci. Technol. 41, 599–605. https://doi.org/10.1021/es061152i

Bañuelos, G., Terry, N., Leduc, D.L., Pilon-Smits, E.A.H., Mackey, B., 2005. Field trial of transgenic Indian mustard plants shows enhanced phytoremediation of selenium-contaminated sediment. Environ. Sci. Technol. 39, 1771–1777. https://doi.org/10.1021/es049035f

Barberon, M., Berthomieu, P., Clairotte, M., Shibagaki, N., Davidian, J.C., Gosti, F., 2008. Unequal functional redundancy between the two Arabidopsis thaliana high-affinity sulphate transporters SULTR1;1 and SULTR1;2. New Phytol. 180, 608–619.

https://doi.org/10.1111/j.1469-8137.2008.02604.x

Belsham, G.J., Barker, D.G., Smith, A.E., 1986. Expression of polyoma virus middle-T antigen in Saccharomyces cerevisiae. Eur. J. Biochem. 156, 413–421. https://doi.org/10.1111/j.1432-1033.1986.tb09598.x

Berardini, T.Z., Reiser, L., Li, D., Mezheritsky, Y., Muller, R., Strait, E., Huala, E., 2015. The arabidopsis information resource: Making and mining the "gold standard" annotated reference plant genome. Genesis 53, 474–485. https://doi.org/10.1002/dvg.22877

Bick, J.A., Leustek, T., 1998. Plant sulfur metabolism - the reduction of sulfate to sulfite. Curr. Opin. Plant Biol. 1, 240–244. https://doi.org/10.1016/S1369-5266(98)80111-8

Bogdanova, N., Hell, R., 1997. Cysteine synthesis in plants: protein-protein interactions of serine acetyltransferase from Arabidopsis thaliana. Plant J. 11, 251–262. https://doi.org/10.1046/j.1365-313X.1997.11020251.x

Bohrer, A.-S., Kopriva, S., Takahashi, H., 2015a. Plastid-cytosol partitioning and integration of metabolic pathways for APS/PAPS biosynthesis in Arabidopsis thaliana. Front. Plant Sci. 5, 1–4. https://doi.org/10.3389/fpls.2014.00751

Bohrer, A.-S., Yoshimoto, N., Sekiguchi, A., Rykulski, N., Saito, K., Takahashi, H., 2015b. Alternative translational initiation of ATP sulfurylase underlying dual localization of sulfate assimilation pathways in plastids and cytosol in Arabidopsis thaliana. Front. Plant Sci. 5, 1–10. https://doi.org/10.3389/fpls.2014.00750

Boldrin, P.F., de Figueiredo, M.A., Yang, Y., Luo, H., Giri, S., Hart, J.J., Faquin, V., Guilherme, L.R.G., Thannhauser, T.W., Li, L., 2016. Selenium promotes sulfur accumulation and plant growth in wheat (Triticum aestivum). Physiol. Plant. 158, 80–91. https://doi.org/10.1111/ppl.12465

Boorer, K.J., Frommer, W.B., Bush, D.R., Kreman, M., Loo, D.D.F., Wright, E.M., 1996. Kinetics and Specificity of a H+/Amino Acid Transporter from Arabidopsis thaliana. J. Biol. Chem. 271, 2213–2220. https://doi.org/10.1074/jbc.271.4.2213

Bosl, M.A., Takaku, K., Oshima, M., Nishimura, S., Taketo, M.M., 1997. Early embryonic lethality caused by targeted disruption of the mouse selenocysteine tRNA gene (Trsp). Proc. Natl. Acad. Sci. U. S. A. 94, 5531–5534. https://doi.org/10.1006/dbio.1996.0208

Both, E.B., Stonehouse, G.C., Lima, L.W., Fakra, S.C., Aguirre, B., Wangeline, A.L., Xiang, J., Yin, H., Jókai, Z., Soós, Á., Dernovics, M., Pilon-Smits, E.A.H., 2020. Selenium tolerance, accumulation, localization and speciation in a Cardamine hyperaccumulator and a non-hyperaccumulator. Sci. Total Environ. 703. https://doi.org/10.1016/j.scitotenv.2019.135041

Cabannes, E., Buchner, P., Broadley, M.R., Hawkesford, M.J., 2011. A Comparison of Sulfate and Selenium Accumulation in Relation to the Expression of Sulfate Transporter Genes in

Astragalus Species. Plant Physiol. 157, 2227–2239. https://doi.org/10.1104/pp.111.183897

Cao, M.J., Wang, Z., Wirtz, M., Hell, R., Oliver, D.J., Xiang, C.-B., 2013. SULTR3;1 is a chloroplast-localized sulfate transporter in Arabidopsis thaliana. Plant J. 73, 607–616. https://doi.org/10.1111/tpj.12059

Cappa, J.J., Cappa, P.J., El Mehdawi, A.F., McAleer, J.M., Simmons, M.P., Pilon-Smits, E.A.H., 2014. Characterization of selenium and sulfur accumulation across the genus Stanleya (Brassicaceae): A field survey and common-garden experiment. Am. J. Bot. 101, 830–839. https://doi.org/10.3732/ajb.1400041

Cappa, J.J., Pilon-Smits, E.A.H., 2014. Evolutionary aspects of elemental hyperaccumulation. Planta 239, 267–275. https://doi.org/10.1007/s00425-013-1983-0

Chen, Z., Zhao, P.-X., Miao, Z.-Q., Qi, G.-F., Wang, Z., Yuan, Y., Ahmad, N., Cao, M.-J., Hell, R., Wirtz, M., Xiang, C.-B., 2019. SULTR3s Function in Chloroplast Sulfate Uptake and Affect ABA Biosynthesis and the Stress Response. Plant Physiol. 180, 593–604. https://doi.org/10.1104/pp.18.01439

Combs, G.F., 2001. Selenium in global food systems. Br. J. Nutr. 85, 517–547. https://doi.org/10.1079/bjn2000280

Dawson, J.C., Anderson, J.W., 1988. Incorporation of cysteine and selenocysteine into cystathionine and selenocystathionine by crude extracts of spinach. Phytochemistry 27, 3453–3460. https://doi.org/10.1016/0031-9422(88)80747-7

De Souza, M.P., Lytle, C.M., Mulholland, M.M., Otte, M.L., Terry, N., 2000. Selenium Assimilation and Volatilization from Dimethylselenoniopropionate by Indian Mustard. Plant Physiol. 122, 1281–1288. https://doi.org/10.1104/pp.122.4.1281

de Valença, A.W., Bake, A., Brouwer, I.D., Giller, K.E., 2017. Agronomic biofortification of crops to fight hidden hunger in sub-Saharan Africa. Glob. Food Sec. 12, 8–14. https://doi.org/10.1016/j.gfs.2016.12.001

Dilworth, G.L., Bandurski, R.S., 1977. Activation of Selenate by Adenosine 5'-Triphosphate Sulphurylase from Saccharomyces cerevisiae. Biochem. J. 163, 521–529. https://doi.org/10.1042/bj1630521

Ding, Y., Zhou, X., Zuo, L., Wang, H., Yu, D., 2016. Identification and functional characterization of the sulfate transporter gene GmSULTR1;2b in soybean. BMC Genomics 17, 1–19. https://doi.org/10.1186/s12864-016-2705-3

El Kassis, E., Cathala, N., Rouached, H., Fourcroy, P., Berthomieu, P., Terry, N., Davidian, J.C., 2007. Characterization of a selenate-resistant Arabidopsis mutant. Root growth as a potential target for selenate toxicity. Plant Physiol. 143, 1231–1241. https://doi.org/10.1104/pp.106.091462

El Mehdawi, A.F., Jiang, Y., Guignardi, Z.S., Esmat, A., Pilon, M., Pilon-Smits, E.A.H., Schiavon, M., 2018. Influence of sulfate supply on selenium uptake dynamics and expression of sulfate/selenate transporters in selenium hyperaccumulator and nonhyperaccumulator Brassicaceae. New Phytol. 217, 194–205. https://doi.org/10.1111/nph.14838

El Mehdawi, A.F., Lindblom, S.D., Cappa, J.J., Fakra, S.C., Pilon-Smits, E.A.H., 2015a. Do selenium hyperaccumulators affect selenium speciation in neighboring plants and soil? An X-Ray Microprobe Analysis. Int. J. Phytoremediation 17, 753–765. https://doi.org/10.1080/15226514.2014.987374

El Mehdawi, A.F., Paschke, M.W., Pilon-Smits, E.A.H., 2015b. Symphyotrichum ericoides populations from seleniferous and nonseleniferous soil display striking variation in selenium accumulation. New Phytol. 206, 231–242. https://doi.org/10.1111/nph.13164

El Mehdawi, A.F., Pilon-Smits, E.A.H., 2012. Ecological aspects of plant selenium hyperaccumulation. Plant Biol. 14, 1–10. https://doi.org/10.1111/j.1438-8677.2011.00535.x

Ellis, D.R., Salt, D.E., 2003. Plants, selenium and human health. Curr. Opin. Plant Biol. 6, 273–279. https://doi.org/10.1016/S1369-5266(03)00030-X

Eustice, D.C., Kull, F.J., Shrift, A., 1981. Selenium Toxicity: Aminoacylation and Peptide Bond Formation with Selenomethionine. Plant Physiol. 67, 1054–1058. https://doi.org/10.1104/pp.67.5.1054

Fisher, B., Yarmolinsky, D., Abdel-Ghany, S., Pilon, M., Pilon-Smits, E.A., Sagi, M., Van Hoewyk, D., 2016. Superoxide generated from the glutathione-mediated reduction of selenite damages the iron-sulfur cluster of chloroplastic ferredoxin. Plant Physiol. Biochem. 106, 228–235. https://doi.org/10.1016/j.plaphy.2016.05.004

Freeman, J.L., Tamaoki, M., Stushnoff, C., Quinn, C.F., Cappa, J.J., Devonshire, J., Fakra, S.C., Marcus, M.A., McGrath, S.P., van Hoewyk, D., Pilon-Smits, E.A.H., 2010. Molecular mechanisms of selenium tolerance and hyperaccumulation in Stanleya pinnata. Plant Physiol. 153, 1630–1652. https://doi.org/10.1104/pp.110.156570

Freeman, J.L., Zhang, L.H., Marcus, M.A., Fakra, S., McGrath, S.P., Pilon-Smits, E.A.H., 2006. Spatial Imaging, Speciation, and Quantification of Selenium in the Hyperaccumulator Plants Astragalus bisulcatus and Stanleya pinnata. Plant Physiol. 142, 124–134. https://doi.org/10.1104/pp.106.081158

Gabel-Jensen, C., Lunøe, K., Gammelgaard, B., 2010. Formation of methylselenol, dimethylselenide and dimethyldiselenide in in vitro metabolism models determined by headspace GC-MS. Metallomics 2, 167–173. https://doi.org/10.1039/b914255j

Galeas, M.L., Klamper, E.M., Bennett, L.E., Freeman, J.L., Kondratieff, B.C., Quinn, C.F.,

Pilon-Smits, E.A.H., 2008. Selenium hyperaccumulation reduces plant arthropod loads in the field. New Phytol. 177, 715–724. https://doi.org/10.1111/j.1469-8137.2007.02285.x

Gietz, R.D., Schiestl, R.H., 2007. High-efficiency yeast transformation using the LiAc / SS carrier DNA / PEG method. Nat. Protoc. 2, 31–35. https://doi.org/10.1038/nprot.2007.13

Gigolashvili, T., Kopriva, S., 2014. Transporters in plant sulfur metabolism. Front. Plant Sci. 5. https://doi.org/10.3389/fpls.2014.00442

Grant, K., Carey, N.M., Mendoza, M., Schulze, J., Pilon, M., Pilon-Smits, E.A.H., Van Hoewyk, D., 2011. Adenosine 5′-phosphosulfate reductase (APR2) mutation in Arabidopsis implicates glutathione deficiency in selenate toxicity. Biochem. J. 438, 325–335. https://doi.org/10.1042/BJ20110025

Guignardi, Z.S., 2017. Studies on selenium hyperaccumulator Stanleya pinnata and nonaccumulator Stanleya elata (Brassicaceae): Functional characterization of selenate transporter SULTR1;2 in yeast and developent of a micropropagation protocol. Colorado State University.

Gupta, S., Gupta, M., 2016. Alleviation of selenium toxicity in Brassica juncea L.: salicylic acid-mediated modulation in toxicity indicators, stress modulators, and sulfur-related gene transcripts. Protoplasma 253, 1515–1528. https://doi.org/10.1007/s00709-015-0908-0

Hall, D.I., Smith, I.K., 1983. Partial Purification and Characterization of Cystine Lyase from Cabbage (Brassica oleracea var capitata). Plant Physiol. 72, 654–658. https://doi.org/10.1104/pp.72.3.654

Hamilton, S.J., 1999. Hypothesis of Historical Effects from Selenium on Endangered Fish in the Colorado River Basin. Hum. Ecol. Risk Assess. 5, 1153–1180. https://doi.org/10.1080/10807039.1999.10518884

Harris, J., Schneberg, K.A., Pilon-Smits, E.A.H., 2014. Sulfur-selenium-molybdenum interactions distinguish selenium hyperaccumulator Stanleya pinnata from non-hyperaccumulator Brassica juncea (Brassicaceae). Planta 239, 479–491. https://doi.org/10.1007/s00425-013-1996-8

Hawrylak-Nowak, B., 2013. Comparative effects of selenite and selenate on growth and selenium accumulation in lettuce plants under hydroponic conditions. Plant Growth Regul. 70, 149–157. https://doi.org/10.1007/s10725-013-9788-5

Hawrylak-Nowak, B., Matraszek, R., Pogorzelec, M., 2015. The dual effects of two inorganic selenium forms on the growth, selected physiological parameters and macronutrients accumulation in cucumber plants. Acta Physiol. Plant. 37. https://doi.org/10.1007/s11738-015-1788-9

Heeg, C., Kruse, C., Jost, R., Gutensohn, M., Ruppert, T., Wirtz, M., Hella, R., 2008. Analysis of

the Arabidopsis O-acetylserine(thiol)lyase Gene Family Demonstrates Compartment-Specific Differences in the Regulation of Cysteine Synthesis. Plant Cell 20, 168–185. https://doi.org/10.1105/tpc.107.056747

Hira, C.K., Partal, K., Dhillon, K.S., 2004. Dietary selenium intake by men and women in high and low selenium areas of Punjab. Public Health Nutr. 7, 39–43. https://doi.org/10.1079/phn2003513

Hirner, A., Ladwig, F., Stransky, H., Okumoto, S., Keinath, M., Harms, A., Frommer, W.B., Koch, W., 2006. Arabidopsis LHT1 is a High-Affinity Transporter for Cellular Amino Acid Uptake in Both Root Epidermis and Leaf Mesophyll. Plant Cell 18, 1931–1946. https://doi.org/10.1105/tpc.106.041012

Hoffmann, P.R., Berry, M.J., 2008. The influence of selenium on immune responses. Mol. Nutr. Food Res. 52, 1273–1280. https://doi.org/10.1002/mnfr.200700330

Hsieh, H.S., Ganther, H.E., 1975. Acid-Volatile Selenium Formation Catalyzed by Glutathione Reductase. Biochemistry 14, 1632–1636. https://doi.org/10.1021/bi00679a014

Huang, Q.Q., Wang, Q., Wan, Y.N., Yu, Y., Jiang, R.F., Li, H.F., 2017. Application of X-ray absorption near edge spectroscopy to the study of the effect of sulphur on selenium uptake and assimilation in wheat seedlings. Biol. Plant. 61, 726–732. https://doi.org/10.1007/s10535-016-0698-z

Huang, Y., Wang, Q., Gao, J., Lin, Z., Bañuelos, G.S., Yuan, L., Yin, X., 2013. Daily Dietary Selenium Intake in a High Selenium Area of Enshi, China. Nutrients 5, 700–710. https://doi.org/10.3390/nu5030700

Jabbar, M.A., Sivasubramanian, N., Nayak, D.P., 1985. Influenza viral (A/WSN/33) hemagglutinin is expressed and glycosylated in the yeast Saccharomyces cerevisiae. Proc. Natl. Acad. Sci. U. S. A. 82, 2019–2023. https://doi.org/10.1073/pnas.82.7.2019

Janowicz, Z.A., Henning, U., Hollenberg, C.P., 1982. Synthesis of Escherichia coli outer membrane OmpA protein in yeasts. Gene 20, 347–358. https://doi.org/10.1016/0378-1119(82)90203-7

Jiang, L., Yang, J., Liu, C., Chen, Z., Yao, Z., Cao, S., 2020. Overexpression of ethylene response factor ERF96 gene enhances selenium tolerance in Arabidopsis. Plant Physiol. Biochem. 149, 294–300. https://doi.org/10.1016/j.plaphy.2020.02.024

Jiang, Y., Schiavon, M., Lima, L.W., Tripti, Jones, R.R., El Mehdawi, A.F., Royer, S., Zeng, Z., Hu, Y., Pilon-Smits, E.A.H., Pilon, M., 2018. Comparison of ATP sulfurylase 2 from selenium hyperaccumulator Stanleya pinnata and non-accumulator Stanleya elata reveals differential intracellular localization and enzyme activity levels. Biochim. Biophys. Acta - Gen. Subj. 1862, 2363–2371. https://doi.org/10.1016/j.bbagen.2018.03.014

Johnson, R.C., Stewart, A.R., Limburg, K.E., Huang, R., Cocherell, D., Feyrer, F., 2020. Lifetime Chronicles of Selenium Exposure Linked to Deformities in an Imperiled Migratory Fish. Environ. Sci. Technol. 54, 2892–2901. https://doi.org/10.1021/acs.est.9b06419

Kataoka, T., Hayashi, N., Yamaya, T., Takahashi, H., 2004a. Root-to-Shoot Transport of Sulfate in Arabidopsis. Evidence for the Role of SULTR3;5 as a Component of Low-Affinity Sulfate Transport System in the Root Vasculature. Plant Physiol. 136, 4198–4204. https://doi.org/10.1104/pp.104.045625

Kataoka, T., Watanabe-Takahashi, A., Hayashi, N., Ohnishi, M., Mimura, T., Buchner, P., Hawkesford, M.J., Yamaya, T., Takahashi, H., 2004b. Vacuolar Sulfate Transporters are Essential Determinants Controlling Internal Distribution of Sulfate in Arabidopsis. Plant Cell 16, 2693–2704. https://doi.org/10.1105/tpc.104.023960

Khamkhash, A., Srivastava, V., Ghosh, T., Akdogan, G., Ganguli, R., Aggarwal, S., 2017. Mining-related selenium contamination in Alaska, and the state of current knowledge. Minerals 7. https://doi.org/10.3390/min7030046

Kikkert, J., Berkelaar, E., 2013. Plant uptake and translocation of inorganic and organic forms of selenium. Arch. Environ. Contam. Toxicol. 65, 458–465. https://doi.org/10.1007/s00244-013-9926-0

Kim, S., Chen, J., Cheng, T., Gindulyte, A., He, J., He, S., Li, Q., Shoemaker, B.A., Thiessen, P.A., Yu, B., Zaslavsky, L., Zhang, J., Bolton, E.E., 2019. PubChem 2019 update: improved access to chemical data. Nucleic Acids Res. 47, D1102–D1109. https://doi.org/10.1093/nar/gky1033

Koprivova, A., Kopriva, S., 2016. Sulfation pathways in plants. Chem. Biol. Interact. 259, 23–30. https://doi.org/10.1016/j.cbi.2016.05.021

LeDuc, D.L., Tarun, A.S., Montes-Bayon, M., Meija, J., Malit, M.F., Wu, C.P., Abdelsamie, M., Chiang, C.-Y., Tagmount, A., Neuhierl, B., Caruso, J., Terry, N., 2004. Overexpression of Selenocysteine Methyltransferase in Arabidopsis and Indian Mustard Increases Selenium Tolerance and Accumulation. Plant Physiol. 135, 377–383. https://doi.org/10.1104/pp.103.026989.effluents

Lenth, R. V, 2016. Least-Squares Means: The R Package lsmeans. J. Stat. Softw. 69, 1–33. https://doi.org/10.18637/jss.v069.i01

Leustek, T., 1996. Molecular genetics of sulfate assimilation in plants. Physiol. Plant. 97, 411–419.

Lewis, B.G., Johnson, C.M., 1974. Selenium in higher plants: The production of dimethyl selenide in cabbage leaves by enzymatic cleavage of Se-methyl selenomethionine selenonium salt. Plant Soil 40, 107–118.

Li, H.F., McGrath, S.P., Zhao, F.J., 2008. Selenium uptake, translocation and speciation in wheat supplied with selenate or selenite. New Phytol. 178, 92–102. https://doi.org/10.1111/j.1469-8137.2007.02343.x

Lima, L.W., Pilon-Smits, E.A.H., Schiavon, M., 2018. Mechanisms of selenium hyperaccumulation in plants: A survey of molecular, biochemical and ecological cues. Biochim. Biophys. Acta - Gen. Subj. 1862, 2343–2353. https://doi.org/10.1016/j.bbagen.2018.03.028

Liu, J., Yang, L., Luan, M., Wang, Y., Zhang, C., Zhang, B., Shi, J., Zhao, F.G., Lan, W., Luan, S., 2015. A vacuolar phosphate transporter essential for phosphate homeostasis in Arabidopsis. Proc. Natl. Acad. Sci. U. S. A. 112, E6571–E6578. https://doi.org/10.1073/pnas.1514598112

Liu, T.-Y., Huang, T.-K., Yang, S.-Y., Hong, Y.-T., Huang, S.-M., Wang, F.-N., Chiang, S.-F., Tsai, S.-Y., Lu, W.-C., Chiou, T.-J., 2016. Identification of plant vacuolar transporters mediating phosphate storage. Nat. Commun. 7. https://doi.org/10.1038/ncomms11095

Lyi, S.M., Heller, L.I., Rutzke, M., Welch, R.M., Kochian, L. V., Li, L., 2005. Molecular and Biochemical Characterization of the Selenocysteine Se-Methyltransferase Gene and Se-Methylselenocysteine Synthesis in Broccoli. Plant Physiol. 138, 409–420. https://doi.org/10.1104/pp.104.056549.evidence

MacFarquhar, J.K., Broussard, D.L., Melstrom, P., Hutchinson, R., Wolkin, A., Martin, C., Burk, R.F., Dunn, J.R., Green, A.L., Hammond, R., Schaffner, W., Jones, T.F., 2010. Acute Selenium Toxicity Associated With a Dietary Supplement. Arch. Intern. Med. 170, 256–261. https://doi.org/10.1001/archinternmed.2009.495

Maimann, S., Hoefgen, R., Hesse, H., 2001. Enhanced cystathionine β-lyase activity in transgenic potato plants does not force metabolite flow towards methionine. Planta 214, 163–170. https://doi.org/10.1007/s004250100651

Martinoia, E., Massonneau, A., Frangne, N., 2000. Transport Processes of Solutes Across the Vacuolar Membrane of Higher Plants. Plant Cell Physiol. 41, 1175–1186. https://doi.org/10.1093/pcp/pcd059

Massonneau, A., Martinoia, E., Dietz, K.-J., Mimura, T., 2000. Phosphate uptake across the tonoplast of intact vacuoles isolated from suspension-cultured cells of Catharanthus roseus (L.) G. Don. Planta 211, 390–395. https://doi.org/10.1007/s004250000297

Matoba, R., Kimura, H., Uchima, E., Shikata, I., Abe, T., Yamada, T., Mitsukuni, Y., Shikata, I., 1986. An autopsy case of acute selenium (selenious acid) poisoning and selenium levels in human tissues. Forensic Sci. Int. 31, 87–92. https://doi.org/10.1016/0379-0738(86)90192-1

McCluskey, T.J., Scarf, A.R., Anderson, J.W., 1986. Enzyme catalysed α,β-elimination of selenocystathionine and selenocystine and their sulphur isologues by plant extracts.

Phytochemistry 25, 2063–2068. https://doi.org/10.1016/0031-9422(86)80067-X

Mikkelsen, R.L., Page, A.L., Bingham, F.T., 1989. Factors Affecting Selenium Accumulation by Agricultural Crops, in: Jacobs, L.W. (Ed.), Selenium in Agriculture and the Environment. Madison, Wisconsin, pp. 65–94. https://doi.org/10.2136/sssaspecpub23.c4

National Academy of Sciences, 2000. Dietary reference intakes for vitamin C, vitamin E, selenium, and carotenoids : a report of the Panel on Dietary Antioxidants and Related Compounds, Subcommittees on Upper Reference Levels of Nutrients and of Interpretation and Use of Dietary Reference In.

Neuhierl, B., Böck, A., 1996. On the mechanism of selenium tolerance in selenium-accumulating plants: Purification and characterization of a specific selenocysteine methyltransferase from cultured cells of Astragalus bisculatus. Eur. J. Biochem. 239, 235–238. https://doi.org/10.1111/j.1432-1033.1996.0235u.x

Ng, B.H., Anderson, J.W., 1979. Light-dependent incorporation of selenite and sulphite into selenocysteine and cysteine by isolated pea chloroplasts. Phytochemistry 18, 573–580. https://doi.org/10.1016/S0031-9422(00)84263-6

Ng, B.H., Anderson, J.W., 1978. Synthesis of selenocysteine by cysteine synthases from selenium accumulator and non-accumulator plants. Phytochemistry 17, 2069–2074. https://doi.org/10.1016/S0031-9422(00)89282-1

Noji, M., Saito, M., Nakamura, M., Aono, M., Saji, H., Saito, K., 2001. Cysteine synthase overexpression in tobacco confers tolerance to sulfur-containing environmental pollutants. Plant Physiol. 126, 973–980. https://doi.org/10.1104/pp.126.3.973

Ohlendorf, H.M., Hothem, R.L., Bunck, C.M., Marois, K.C., 1990. Bioaccumulation of Selenium in Birds at Kesterson Reservoir, California. Arch. Environ. Contam. Toxicol. 19, 495–507. https://doi.org/10.1007/BF01059067

Peterson, P.J., Butler, G.W., 1962. The uptake and assimilation of selenite by higher plants. Aust. J. Biol. Sci. 15. https://doi.org/10.1071/bi9620126

Pilon-Smits, E.A., Quinn, C.F., Tapken, W., Malagoli, M., Schiavon, M., 2009. Physiological functions of beneficial elements. Curr. Opin. Plant Biol. 12, 267–274. https://doi.org/10.1016/j.pbi.2009.04.009

Pilon-Smits, E.A.H., Garifullina, G.F., Abdel-Ghany, S., Kato, S.-I., Mihara, H., Hale, K.L., Burkhead, J.L., Esaki, N., Kurihara, T., Pilon, M., 2002. Characterization of a NifS-Like Chloroplast Protein from Arabidopsis. Implications for Its Role in Sulfur and Selenium Metabolism. Plant Physiol. 130, 1309–1318. https://doi.org/10.1104/pp.010280

Pilon-Smits, E.A.H., Hwang, S., Lytle, C.M., Zhu, Y., Tai, J.C., Bravo, R.C., Chen, Y., Leustek, T., Terry, N., 1999. Overexpression of ATP Sulfurylase in Indian Mustard Leads to

Increased Selenate Uptake, Reduction, and Tolerance. Plant Physiol. 119, 123–132. https://doi.org/10.1104/pp.119.1.123

Pottosin, I., Shabala, S., 2016. Transport Across Chloroplast Membranes: Optimizing Photosynthesis for Adverse Environmental Conditions. Mol. Plant 9, 356–370. https://doi.org/10.1016/j.molp.2015.10.006

Presser, T.S., Luoma, S.N., 2006. Forecasting selenium discharges to the San Francisco Bay-Delta Estuary ecological effects of a proposed San Luis drain extension, USGS Professional paper 1646.

Ranjard, L., Prigent-Combaret, C., Nazaret, S., Cournoyer, B., 2002. Methylation of Inorganic and Organic Selenium by the Bacterial Thiopurine Methyltransferase. J. Bacteriol. 184, 3146–3149. https://doi.org/10.1128/JB.184.11.3146-3149.2002

Raspor, P., Fujs, Š., Banszky, L., Maraz, A., Batič, M., 2003. The involvement of ATP sulfurylase in Se(VI) and Cr(VI) reduction processes in the fission yeast Schizosaccharomyces pombe. Appl. Microbiol. Biotechnol. 63, 89–95. https://doi.org/10.1007/s00253-003-1336-1

Ravanel, S., Block, M.A., Rippert, P., Jabrin, S., Curien, G., Rébeillé, F., Douce, R., 2004. Methionine Metabolism in Plants: Chloroplasts are autonomous for de novo methionine synthesis and can import S-adenosylmethionine from the cytosol. J. Biol. Chem. 279, 22548–22557. https://doi.org/10.1074/jbc.M313250200

Ravanel, S., Gakière, B., Job, D., Douce, R., 1998. The specific features of methionine biosynthesis and metabolism in plants. Proc. Natl. Acad. Sci. U. S. A. 95, 7805–7812. https://doi.org/10.1073/pnas.95.13.7805

Rayman, M.P., 2012. Selenium and human health. Lancet 379, 1256–1268. https://doi.org/10.1016/S0140-6736(11)61452-9

Regina, B.F., Gladyshev, V.N., Arnér, E.S., Berry, M.J., Bruford, E.A., Burk, R.F., Carlson, B.A., Castellano, S., Chavatte, L., Conrad, M., Copeland, P.R., Diamond, A.M., Driscoll, D.M., Ferreiro, A., Flohé, L., Green, F.R., Guigó, R., Handy, D.E., Hatfield, D.L., Hesketh, J., Hoffmann, P.R., Holmgren, A., Hondal, R.J., Howard, M.T., Huang, K., Kim, H.Y., Kim, I.Y., Köhrle, J., Krol, A., Kryukov, G. V., Lee, B.J., Lee, B.C., Lei, X.G., Liu, Q., Lescure, A., Lobanov, A. V., Loscalzo, J., Maiorino, M., Mariotti, M., Prabhu, K.S., Rayman, M.P., Rozovsky, S., Salinas, G., Schmidt, E.E., Schomburg, L., Schweizer, U., Simonović, M., Sunde, R.A., Tsuji, P.A., Tweedie, S., Ursini, F.F., Whanger, P.D., Zhang, Y., 2016. Selenoprotein Gene Nomenclature. J. Biol. Chem. 291, 24036–24040. https://doi.org/10.1074/jbc.M116.756155

Richards, O.W., 1928. Potentially unlimited multiplication of yeast with constant environment, and the limiting of growth by changing environment. Gen. Physiol. 525–538.

Romanos, M.A., Scorer, C.A., Clare, J.J., 1992. Foreign Gene Expression in Yeast: A Review. Yeast 8, 1–66.

Rouached, H., Berthomieu, P., El Kassis, E., Cathala, N., Catherinot, V., Labesse, G., Davidian, J.C., Fourcroy, P., 2005. Structural and functional analysis of the C-terminal STAS (sulfate transporter and anti-sigma antagonist) domain of the Arabidopsis thaliana sulfate transporter SULTR1.2. J. Biol. Chem. 280, 15976–15983. https://doi.org/10.1074/jbc.M501635200

Rouached, H., Wirtz, M., Alary, R., Hell, R., Arpat, A.B., Davidian, J.C., Fourcroy, P., Berthomieu, P., 2008. Differential Regulation of the Expression of Two High-Affinity Sulfate Transporters, SULTR1.1 and SULTR1.2, in Arabidopsis1. Plant Physiol. 147, 897–911. https://doi.org/10.1104/pp.108.118612

Schiavon, M., Pilon-Smits, E.A.H., 2017. The fascinating facets of plant selenium accumulation – biochemistry, physiology, evolution and ecology. New Phytol. 213, 1582–1596. https://doi.org/10.1111/nph.14378

Schmidt, R.L., Simonović, M., 2012. Synthesis and decoding of selenocysteine and human health. Croat. Med. J. 53, 535–550. https://doi.org/10.3325/cmj.2012.53.535

See, K.A., Lavercombe, P.S., Dillon, J., Ginsberg, R., 2006. Accidental death from acute selenium poisoning. Med. J. Aust. 185, 388–389. https://doi.org/10.5694/j.1326-5377.2007.tb01018.x

Setya, A., Murillo, M., Leustek, T., 1996. Sulfate reduction in higher plants: Molecular evidence for a novel 5′-adenylylsulfate reductase. Proc. Natl. Acad. Sci. U. S. A. 93, 13383–13388. https://doi.org/10.1073/pnas.93.23.13383

Shibagaki, N., Grossman, A.R., 2006. The role of the STAS domain in the function and biogenesis of a sulfate transporter as probed by random mutagenesis. J. Biol. Chem. 281, 22964–22973. https://doi.org/10.1074/jbc.M603462200

Shibagaki, N., Grossman, A.R., 2004. Probing the function of STAS domains of the Arabidopsis sulfate transporters. J. Biol. Chem. 279, 30791–30799. https://doi.org/10.1074/jbc.M403248200

Shibagaki, N., Rose, A., McDermott, J.P., Fujiwara, T., Hayashi, H., Yoneyama, T., Davies, J.P., 2002. Selenate-resistant mutants of Arabidopsis thaliana identify Sultr1;2, a sulfate transporter required for efficient transport of sulfate into roots. Plant J. 29, 475–486. https://doi.org/10.1046/j.0960-7412.2001.01232.x

Shinmachi, F., Buchner, P., Stroud, J.L., Parmar, S., Zhao, F.J., Mcgrath, S.P., Hawkesford, M.J., Common, W., Al, H., S, U.K.F., 2010. Influence of Sulfur Deficiency on the Expression of Specific Sulfate Transporters and the Distribution of Sulfur , Selenium , and Molybdenum in Wheat. Plant Physiol. 153, 327–336. https://doi.org/10.1104/pp.110.153759

Sikorski, R.S., Hieter, P., 1989. A System of Shuttle Vectors and Yeast Host Strains Designed for Efficient Manipulation of DNA in Saccharomyces ceratisiae. Genetics 122, 19–27.

Song, Z., Shao, H., Huang, H., Shen, Y., Wang, L., Wu, F., Han, D., Song, J., Jia, H., 2017. Overexpression of the phosphate transporter gene OsPT8 improves the Pi and selenium contents in Nicotiana tabacum. Environ. Exp. Bot. 137, 158–165. https://doi.org/10.1016/j.envexpbot.2017.02.011

Sors, T.G., Ellis, D.R., Gun, N.N., Lahner, B., Lee, S., Leustek, T., Pickering, I.J., Salt, D.E., 2005a. Analysis of sulfur and selenium assimilation in Astragalus plants with varying capacities to accumulate selenium. Plant J. 42, 785–797. https://doi.org/10.1111/j.1365-313X.2005.02413.x

Sors, T.G., Ellis, D.R., Salt, D.E., 2005b. Selenium uptake, translocation, assimilation and metabolic fate in plants. Photosynth. Res. 86, 373–389. https://doi.org/10.1007/s11120-005-5222-9

Sun, J., Stowers, C.C., Boczko, E.M., Li, D., 2010. Measurement of the volume growth rate of single budding yeast with the MOSFET-based microfluidic Coulter counter. Lab Chip 10, 2986–2993. https://doi.org/10.1039/c005029f

Tagmount, A., Berken, A., Terry, N., 2002. An Essential Role of S-Adenosyl-L-Methionine:L-Methionine S-Methyltransferase in Selenium Volatilization by Plants. Methylation of Selenomethionine to Selenium-Methyl-L-Selenium- Methionine, the Precursor of Volatile Selenium. Plant Physiol. 130, 847–856. https://doi.org/10.1104/pp.001693

Takahashi, H., Watanabe-Takahashi, A., Smith, F.W., Blake-Kalff, M., Hawkesford, M.J., Saito, K., 2000. The roles of three functional sulphate transporters involved in uptake and translocation of sulphate in Arabidopsis thaliana. Plant J. 23, 171–182. https://doi.org/10.1046/j.1365-313X.2000.00768.x

Tamaoki, M., Freeman, J.L., Pilon-Smits, E.A.H., 2008. Cooperative Ethylene and Jasmonic Acid Signaling Regulates Selenite Resistance in Arabidopsis. Plant Physiol. 146, 1219–1230. https://doi.org/10.1104/pp.107.110742

Taylor, R.G., Walker, D.C., Mclnnes, R.R., 1993. E.coli host strains significantly affect the quality of small scale plasmid DNA preparations used for sequencing. Nucleic Acids Res. 21, 1677–1678. https://doi.org/10.1093/nar/21.7.1677

Ursini, F., Heim, S., Kiess, M., Maiorino, M., Roveri, A., Wissing, J., Flohé, L., 1999. Dual function of the selenoprotein PHGPx during sperm maturation. Science (80-.). 285, 1393–1396. https://doi.org/10.1126/science.285.5432.1393

Van Hoewyk, D., 2013. A tale of two toxicities: malformed selenoproteins and oxidative stress both contribute to selenium stress in plants. Ann. Bot. 112, 965–972.

https://doi.org/10.1093/aob/mct163

Van Hoewyk, D., Garifullina, G.F., Ackley, A.R., Abdel-Ghany, S.E., Marcus, M.A., Fakra, S., Ishiyama, K., Inoue, E., Pilon, M., Takahashi, H., Pilon-Smits, E.A.H., 2005. Overexpression of AtCpNifS Enhances Selenium Tolerance and Accumulation in Arabidopsis. Plant Physiol. 139, 1518–1528. https://doi.org/10.1104/pp.105.068684

Van Hoewyk, D., Takahashi, H., Inoue, E., Hess, A., Tamaoki, M., Pilon-Smits, E.A.H., 2008. Transcriptome analyses give insights into selenium-stress responses and selenium tolerance mechanisms in Arabidopsis. Physiol. Plant. 132, 236–253. https://doi.org/10.1111/j.1399-3054.2007.01002.x

Van Huysen, T., Abdel-ghany, S., Hale, K.L., LeDuc, D., Terry, N., Pilon-Smits, E.A.H., 2003. Overexpression of cystathionine- c -synthase enhances selenium volatilization in Brassica juncea. Planta 218, 71–78. https://doi.org/10.1007/s00425-003-1070-z

Vinceti, M., Filippini, T., Cilloni, S., Bargellini, A., Vergoni, A.V., Tsatsakis, A., Ferrante, M., 2017. Health risk assessment of environmental selenium: Emerging evidence and challenges (Review). Mol. Med. Rep. 15, 3323–3335. https://doi.org/10.3892/mmr.2017.6377

Wang, J., Cappa, J.J., Harris, J.P., Edger, P.P., Zhou, W., Pires, J.C., Adair, M., Unruh, S.A., Simmons, M.P., Schiavon, M., Pilon-Smits, E.A.H., 2018. Transcriptome-wide comparison of selenium hyperaccumulator and nonaccumulator Stanleya species provides new insight into key processes mediating the hyperaccumulation syndrome. Plant Biotechnol. J. 16, 1582–1594. https://doi.org/10.1111/pbi.12897

Wang, P., Menzies, N.W., Lombi, E., McKenna, B.A., James, S., Tang, C., Kopittke, P.M., 2015. Synchrotron-based X-ray absorption near-edge spectroscopy imaging for laterally resolved speciation of selenium in fresh roots and leaves of wheat and rice. J. Exp. Bot. 66, 4795–4806. https://doi.org/10.1093/jxb/erv254

White, P.J., 2018. Selenium metabolism in plants. Biochim. Biophys. Acta - Gen. Subj. 1862, 2333–2342. https://doi.org/10.1016/j.bbagen.2018.05.006

White, P.J., Bowen, H.C., Marshall, B., Broadley, M.R., 2007. Extraordinarily High Leaf Selenium to Sulfur Ratios Define 'Se-accumulator' Plants. Ann. Bot. 100, 111–118. https://doi.org/10.1093/aob/mcm084

White, P.J., Bowen, H.C., Parmaguru, P., Fritz, M., Spracklen, W.P., Spiby, R.E., Meacham, M.C., Mead, A., Harriman, M., Trueman, L.J., Smith, B.M., Thomas, B., Broadley, M.R., 2004. Interactions between selenium and sulphur nutrition in Arabidopsis thaliana. J. Exp. Bot. 55, 1927–1937. https://doi.org/10.1093/jxb/erh192

World Health Organization, 1996. Trace elements in human nutrition and health. Geneva.

Xue, T., Hartikainen, H., Piironen, V., 2001. Antioxidative and growth-promoting effect of selenium on senescing lettuce. Plant Soil 237, 55–61. https://doi.org/10.1023/A:1013369804867

Yoshimoto, N., Inoue, E., Saito, K., Yamaya, T., Takahashi, H., 2003. Phloem-Localizing Sulfate Transporter, Sultr1;3, Mediates Re-Distribution of Sulfur from Source to Sink Organs in Arabidopsis. Plant Physiol. 131, 1511–1517. https://doi.org/10.1104/pp.014712.plasmamembranes

Yoshimoto, N., Takahashi, H., Smith, F.W., Yamaya, T., Saito, K., 2002. Two distinct high-affinity sulfate transporters with different inducibilities mediate uptake of sulfate in Arabidopsis roots. Plant J. 29, 465–473. https://doi.org/10.1046/j.0960-7412.2001.01231.x

Zhang, J., Taylor, E.W., Bennett, K., Saad, R., Rayman, M.P., 2020. Association between regional selenium status and reported outcome of COVID-19 cases in China. Am. J. Clin. Nutr. 1–3. https://doi.org/10.1093/ajcn/nqaa095

Zhang, L., Hu, B., Li, W., Che, R., Deng, K., Li, H., Yu, F., Ling, H., Li, Y., Chu, C., 2014. OsPT2, a phosphate transporter, is involved in the active uptake of selenite in rice. New Phytol. 201, 1183–1191. https://doi.org/10.1111/nph.12596

Zhang, L.H., Abdel-Ghany, S.E., Freeman, J.L., Ackley, A.R., Schiavon, M., Pilon-Smits, E.A.H., 2006. Investigation of selenium tolerance mechanisms in Arabidopsis thaliana. Physiol. Plant. 128, 212–223. https://doi.org/10.1111/j.1399-3054.2006.00739.x

Zhang, Y., Gladyshev, V.N., 2009. Comparative genomics of trace elements: Emerging dynamic view of trace element utilization and function. Chem. Rev. 109, 4828–4861. https://doi.org/10.1021/cr800557s

Zhao, X.Q., Mitani, N., Yamaji, N., Shen, R.F., Ma, J.F., 2010. Involvement of Silicon Influx Transporter OsNIP2;1 in Selenite Uptake in Rice. Plant Physiol. 153, 1871–1877. https://doi.org/10.1104/pp.110.157867

Zhou, Y., Tang, Q., Wu, M., Mou, D., Liu, H., Wang, S., Zhang, C., Ding, L., Luo, J., 2018. Comparative transcriptomics provides novel insights into the mechanisms of selenium tolerance in the hyperaccumulator plant Cardamine hupingshanensis. Sci. Rep. 8. https://doi.org/10.1038/s41598-018-21268-2

Zhou, Z.S., Smith, A.E., Matthews, R.G., 2000. L-Selenohomocysteine: One-Step Synthesis from L-Selenomethionine and Kinetic Analysis as Substrate for Methionine Synthases. Bioorganic Med. Chem. Lett. 10, 2471–2475. https://doi.org/10.1016/S0960-894X(00)00498-4

CHAPTER 2: CLONING AND FUNCTIONAL CHARACTERIZATION IN YEAST OF POTENTIAL SELENATE TRANSPORTERS FROM HYPERACCUMULATOR STANLEYA PINNATA (BRASSICACEAE)

2.1 Summary

Some plant species, known as selenium (Se) hyperaccumulators (HAs), are able to take up large quantities of Se from the soil resulting in tissue concentrations many times higher than other native vegetation on the same site. Selenium is chemically similar to sulfur (S) and is taken up non-specifically via the same transporter. While the Se:S ratio in most plants tends to reflect that of their growth substrate, HAs show evidence of Se enrichment (an elevated Se:S ratio), suggesting the presence of transporters with enhanced Se specificity. The mechanism for this Se uptake capability is investigated in this study. We hypothesize that in hyperaccumulators one or more sulfate transport proteins have evolved greater preference for the Se analog, selenate. This study focuses on putative root-to-shoot sulfate/selenate transport proteins SpSULTR2;1 and SpSULTR3;5 from Se hyperaccumulator *Stanleya pinnata* (Brassicaceae). The coding regions of transcripts for these proteins were amplified via reverse transcription polymerase chain reaction, cloned in a yeast expression vector and sequenced. Both proteins showed the N-terminal cytosolic domain, 12 membrane-spanning domains, and C-terminal cytosolic STAS (Sulphate Transporter and Anti-Sigma factor antagonist) domains that are characteristic of plant SULTRs. SpSULTR2;1 and SpSULTR3;5 were assayed for selenate specificity by quantifying their relative selenate and sulfate uptake capacities in baker's yeast (*Saccharomyces cerevisiae*). This assay was complemented with selenate-dependent growth curves in liquid media and a selenate tolerance assay on solid media. Both SpSULTR2;1 and SpSULTR3;5 were expressed by the yeast, determined by dot-blot immunoassay. Yeast expressing SpSULTR2;1 demonstrated a

slight but non-significant increase in Se concentration relative to the yeast with the empty vector control in a 1-hour uptake assay when exposed to 1 mM selenate, but not when exposed to 0.1 mM selenate. SpSULTR3;5 was not able to increase the selenate concentration in the yeast relative to the control in the uptake assay. Yeast expressing SpSULTR2;1 or SpSULTR3;5 demonstrated similar selenate tolerance to controls. Expression of SpSULTR3;5 or SpSULTR2;1 also did not significantly affect growth relative to the control in liquid media. In conclusion, more studies are needed to determine with certainty whether SpSULTR2;1 or SpSULTR3;5 have selenate-specific transport capability.

2.2 Introduction

The element selenium (Se) is not an essential plant nutrient (Ellis and Salt, 2003; White, 2018; Zhang and Gladyshev, 2009), and there are to date no known Se-specific transport proteins in plants. Nevertheless, plants often contain low concentrations of Se. Most Se found in plant tissues is taken up in the roots as selenate (SeO_4^{2-}) via sulfate (SO_4^{2-}) transport proteins (SULTRs), due to the structural similarity of the two ions (Anderson, 1993). It is hypothesized that SULTRs are also responsible for distributing selenate throughout the plant (White, 2018). This usually presents a challenge to plants exposed to Se, because in high concentrations, Se causes oxidative stress and disruption of protein function, leading to chlorosis and stunted growth (Van Hoewyk, 2013). However, some species have adapted to not only tolerate, but thrive, on soils naturally containing high concentrations of Se. These species, called Se hyperaccumulators (HAs), preferentially take up Se over S and concentrate Se at concentrations greater than 1,000 mg/kg of their dry weight (Cappa et al., 2014). Research has revealed many of the steps in the metabolic pathways these species use to neutralize the toxic effects of Se (for a

review, see Trippe III and Pilon-Smits, 2021). However, the mechanism by which these plants selectively transport Se remains unknown.

It is possible that HAs have gained the ability to selectively transport Se because one or more of their SULTR proteins has evolved greater specificity for selenate relative to sulfate. Recent transcriptomic analyses support this possibility. A comparative analysis of the Se HA *Stanleya pinnata* (Brassicaceae) and non-HA sister species *Stanleya elata* found that the HA more highly expressed SULTRs predicted to have a wide variety of sulfate and selenate transport roles, including root uptake, root-to-shoot translocation, vacuolar efflux, plastid import, and phloem remobilization (Wang et al., 2018). If one or more of these SULTRS has evolved greater selenate specificity, they could facilitate hyperaccumulation and distribution of Se in *S. pinnata*. The first HA SULTR to be tested for selenate preference was SpSULTR1;2, a *S. pinnata* homolog to the *Arabidopsis thaliana* SULTR1;2. This SULTR represented a logical starting point, because it is the main root uptake SULTR in *Arabidopsis thaliana* under S-replete conditions (Barberon et al., 2008), and thus is the primary location where an HA could preferentially import Se. Furthermore, *SpSultr1;2* was more highly expressed at the mRNA level than any other *Sultr* in *S. pinnata* (Wang et al., 2018). The *SpSultr1;2* coding sequence (CDS) was cloned into the sulfate uptake deficient yeast (*Saccharomyces cerevisiae*) mutant YSD1 and expressed in liquid culture. Cultures were supplemented with sulfate and competing selenate in a range of concentrations for one hour. No increased Se:S ratio was found within yeast expressing SULTR1;2 as compared to the control (Guignardi, 2017). This indicates that, at least in *S. pinnata*, SULTR1;2 may not bear the full or primary responsibility for preferential accumulation of Se.

The study described here considers a second logical possibility, that the putative root-to-shoot sulfate translocators SpSULTR2;1 or SpSULTR3;5 (Sp for *Stanleya pinnata*) contribute to Se-specific accumulation in the shoots of *S. pinnata*. SULTR2;1 and SULTR3;5 are known to cooperatively facilitate such root-to-shoot translocation of sulfate in plants (Cao et al., 2013; Kataoka et al., 2004), and both were more highly expressed at the mRNA level under selenate-supplied conditions in the roots of *S. pinnata* than the roots of non-HA *S. elata* (Wang et al., 2018). Generally, the high Se:S ratio that is characteristic of Se hyperaccumulators is most apparent in the shoot (Cabannes et al., 2011). Therefore, if SULTR1;2 does not differentiate between selenate and sulfate, it is possible that high Se concentrations are only achieved in the shoot by the preferential translocation of selenate.

We tested the hypothesis that either SULTR2;1 or SULTR3;5 has evolved higher selenate specificity in HA *S. pinnata* by assaying their relative Se and S uptake capacities in a yeast model system. First, we amplified, cloned, and sequenced the coding sequences for SpSULTR2;1 and SpSULTR3;5 and compared them to the homologous sequences from *A. thaliana*. We noted non-conservative amino acid substitutions which may contribute to altered functionality in the SULTRs. The C-terminal STAS (Sulfate Transport and Anti-Sigma factor antagonist) domain of each SULTR is a region of interest, because research has demonstrated that this region plays an important role in the sulfate uptake kinetics of *Arabidopsis thaliana* SULTRs (Shibagaki and Grossman, 2004). Special attention is paid to STAS domain mutations in the discussion.

Next, we expressed these two SULTRs from *S. pinnata* in commonly used yeast strain YPH500 and tested Se uptake capacities via one-hour uptake studies in a range of sulfate and selenate concentrations. For comparison, we also tested SULTR1;2 from *S. pinnata* in this strain.

We examined Se and S concentrations in the yeast by inductively coupled plasma mass spectrometry (ICP-MS). In addition, we constructed growth curves for the transformed yeast in the presence of various selenate concentrations and performed selenate tolerance assays of the transformed yeast on agar media.

2.3 Methods

2.3.1 Cloning of SULTR2;1 and SULTR3;5 cDNA from *S. pinnata*

Previously generated cDNA from the root tissue of *S. pinnata* (Wang et al., 2018) was used as template for the amplification of SULTR2;1 and SULTR3;5 coding sequences. Primers were designed using previously generated annotated transcriptome data for *S. pinnata* (Wang et al., 2018) If *S. pinnata* transcriptomic sequences did not provide sufficient coverage of the 5' or 3' ends of the SULTR CDS, primers were instead designed from the corresponding sequence from *Brassica napus*, a relative of *S. pinnata*. Primer details may be found in Table A1.1. All primers were synthesized by Integrated DNA Technologies (Coralville, IA). SULTRs were then amplified by PCR using the high-fidelity polymerase Phusion HF Taq (New England Biolabs, Ipswich, MA). PCR protocols may be found in Table A1.2. Amplified SULTRs were then isolated via agarose gel electrophoresis and extracted using the Qiaquick Gel Extraction Kit (Qiagen, Germantown, MD).

The purified SULTRs were then double-digested with EcoR1-HF and Pac1 in CutSmart buffer (New England Biolabs). Digestion procedures may be found in Table A1.3. A modified pYES2 plasmid (Invitrogen, Carlsbad, CA) was double-digested in the same manner. pYES2 is designed for selection in both *S. cerevisiae* and *E. coli*, and galactose-inducible expression of heterologous genes in *S. cerevisiae*. The previously generated modified version of pYES2 used

here (Guignardi, 2017) contained *S. pinnata* SULTR1;2, ligated on the 5' end into an EcoRI restriction site and on the 3' end into a PacI restriction site. Downstream of the PacI restriction site, the modified pYES2 also contained a Myc tag, followed by a 6xHis tag, and a stop codon. Figure 2.1 diagrams the pYES2 plasmid with the SULTR1;2 insert as an example of the modified plasmid structure. The added C-terminal tags were found to have no effect on the sulfate or selenate transport functionality of the encoded SULTR when expressed in yeast (Guignardi, 2017). Therefore, the tags were retained in these experiments as well. After digestion, the SULTRs and pYES2 were again isolated and extracted, using the method described above. Then, the SULTRs were ligated separately into pYES2 using T4 Ligase (New England Biolabs). Ligation protocol details may be found in Table A1.4. The resulting plasmids are hereafter referred to by specific names, differentiated by the SULTR they contain. They are: pYES2_SpSULTR1;2 (previously generated), pYES2_SpSULTR2;1, pYES2_SpSULTR3;5, and pYES2 (this is the empty vector).

2.3.2 Amplification of Modified pYES2 Plasmids with SULTRs in *E. coli*

Aliquots of the competent *E. coli* strain DH5-α (Taylor et al., 1993) were each transformed via the heat shock method with one of the modified pYES2 plasmids or the unmodified empty vector. Cells were spread-plated onto LB agar plates with 50 mg/mL ampicillin for selection of successfully transformed colonies. The recipes for all nutritional media used in this study may be found in Table A1.7. Plates were incubated at 37°C for 16 hours, after which they were checked for colony growth. A portion of each colony was streaked onto fresh selective plates, and the rest of the colony was used to inoculate 5 mL of selective LB broth with 50 mg/mL ampicillin. The inoculated broth was incubated in 15 mL culture tubes at 37°C, shaking at 200 rpm, for 16 hours. Plasmids were then extracted from the *E. coli* cultures

using the Qiaprep Spin Miniprep Kit (Qiagen). Presence and correct orientation of the gene insert were confirmed by PCR, using the pYES2 T7 forward primer (Invitrogen) and the one-quarter reverse primer for the relevant gene (see Table A1.1 for primer details).

2.3.3 Sequencing of SULTR2;1 and SULTR3;5 Coding Regions

Sequencing primers were generated such that each SULTR coding region was covered with four pairs of forward and reverse primers (see Table A1.1). Each of these eight SULTR-specific primers, plus the pYES2 T7 forward primer, were used to sequence the SULTR genes within the pYES2 plasmid. Sanger plasmid sequencing was performed by Genewiz (South Plainfield, NJ), with samples prepared per Genewiz requirements.

Sequence results were imported to the software program Geneious Prime (Biomatters, Ltd., Auckland, NZ) as FASTA files with corresponding chromatograms. Sequences were trimmed until at least 80% of base calls were rated as high quality. Sequences were then aligned using the homologous *B. napus* SULTR as a scaffold. 100% coverage was achieved for both SULTRs. Sequences were then translated to determine the corresponding amino acid sequences (shown in Table A1.6).

Note that there was one ambiguity associated with an amino acid substitution in *S. pinnata* SULTR3;5. Plasmid isolated from one colony was found to encode a leucine at residue 231, while plasmid isolated from another colony encoded an isoleucine at that position. Due to resource limitations, we were unable to return to the cDNA to produce new copies to sequence. Therefore, we chose to proceed with the leucine version of the gene, as that is the residue at the same position in related species *B. napus* (the residue is an isoleucine in the more distant relative *Arabidopsis thaliana*). In the *S. pinnata* sequence in Table A1.6, this leucine is highlighted and bolded.

2.3.4 Transformation of SULTRs into YPH-500α Yeast

The haploid yeast strain YPH-500α (Sikorski and Hieter, 1989) was streaked from glycerol storage at -80°C onto yeast peptone dextrose (YPD) agar petri plates, and grown at 30°C for 48 hours. At that time, the petri plates were sealed with wax and stored at 4°C. In order to propagate yeast, single colonies were isolated from the initial plate and streaked onto a new YPD plate every four weeks. YPH-500α yeast was then transformed with the modified pYES2 plasmids using a lithium acetate transformation procedure modified from the 2007 protocol published by Gietz and Schiestl (Gietz and Schiestl, 2007). The full modified protocol may be found in Table A1.5. Transformed yeast was streaked onto synthetic defined media plates without uracil, using 2% dextrose as a carbon source (SD -Ura +Dex plates). Direct PCR of transformed yeast was performed to ascertain both the presence and orientation of the pYES2 gene inserts. The resulting yeast lines are hereafter referred to by specific names, differentiated by the SULTR they contain. They are: SpSULTR1;2 (from previously generated pYES2 with SULTR1;2 insert from *S. pinnata*), SpSULTR2;1, SpSULTR3;5, and pYES2 (this line has the plasmid with no SULTR transgene).

2.3.5 Assay for Protein Expression

Yeast lines SpSULTR1;2, SpSULTR2;1, SpSULTR3;5, and pYES2 were grown in 5 mL SD -Ura + Gal broth at 30°C and shaking at 200 rpm until they reached an OD_{600} of 1.0. Then, the cultures were centrifugated at 2,200 g for 5 minutes, and the supernatant was removed. The cell pellets were re-suspended in 1 ml sterile H_2O and moved to a sterile microcentrifuge tube. The samples were again centrifuged as previously, and the supernatant was removed. The cell pellets were placed on ice. 100 µL of blue SDS-PAGE sample buffer and 100 µL of acid-washed glass beads were added to each sample tube, and cell pellets were re-suspended by vortexing.

Samples were then frozen overnight at -80°C. Samples were thawed the next morning and vortexed for 3 rounds of 30 seconds each, followed by a 5 min incubation at 95°C. Samples were returned to ice for 30 sec, vortexed for 30 sec, and then spun in a microcentrifuge at maximum speed for 15 sec.

To determine presence of tagged SULTRs in the protein samples, 5 µL of total protein was pipetted directly onto a nitrocellulose membrane. The nitrocellulose was allowed to air-dry and then briefly washed in TBS with TWEEN® 20 (TBS+T). This was followed by 30 minutes of blocking in 20 mL of a 5% milk solution in TBS+T. The blot was then washed for 4x5 minutes in 10 mL TBS+T, followed by 2-hour incubation in an anti-Myc mouse primary antibody (Thermofisher). The blot was again washed for 4x5 minutes in 10 mL TBS+T, followed by incubation with an anti-mouse horseradish peroxidase secondary antibody. The blot was once more washed for 4x5 min in 10 mL TBS+T, followed by 5 minutes in TBS without TWEEN® 20. After this final wash, the nitrocellulose membrane was exposed to a 10 mL solution of NBT-BCIP (one tablet dissolved in 10 mL deionized water) for 5 minutes. The membrane was then washed in deionized water, allowed to air-dry, and photographed. Figure 2.2 shows the result of this blot.

2.3.6 Selenate Tolerance Assay

Transformed YPH-500α yeast was tested for tolerance to a range of selenate concentrations on agar plates. Cultures of yeast strains SpSULTR1;2, SpSULTR2;1, SpSULTR3;5, and pYES2 were first grown for 48 hours in SD -Ura +Gal broth. These cell cultures were normalized to an optical density at 600 nm wavelength (OD_{600}) of 1.0 using a Beckman DU 530 spectrophotometer (Beckman Coulter Life Sciences, Indianapolis, IN). Then, 10-fold serial dilutions of each overnight culture were prepared to a final OD_{600} of 10^{-5}. 2 µl of

each serial dilution was plated on synthetic defined media plates without uracil, using 2% galactose as a carbohydrate source (SD -Ura +Gal plates) in order to maintain active transcription of the SULTRs. These plates each contained approximately 4 mM sulfate, and were supplemented with selenate, in 500 µM increments, from 0 to 5 mM (by which concentration growth was fully inhibited in all yeast lines). The cells were incubated at 30°C for 120 hours. At 72 hours and again at 120 hours, plates were photographed against a black background. The growth of each colony was assessed by visual observation of the spot plate photographs. Assessment of selenate tolerance was conducted once.

2.3.7 Yeast Growth Curve Assay

To determine the effect of selenate on the growth of yeast cells in liquid culture, strains SpSULTR1;2, SpSULTR2;1, SpSULTR3;5, and pYES2 were grown in the presence of various concentrations of selenate and their growth curve was plotted over time. Aliquots of 100 mL of SD -Ura +Dex broth (with 4 mM sulfate) were first inoculated to a starting OD_{600} of 0.02 with each yeast strain. These were grown at 30°C in a shaking incubator set to 200 rpm for 36 hours. The cultures were then centrifuged for 5 min at 1,500 g. The supernatant was removed, and the cell pellet was resuspended, with vortexing, in 5 mL of SD -Ura +Gal broth (with 4mM sulfate). The spin and resuspension in SD -Ura +Gal broth was repeated once. Then, aliquots of 100 mL of SD -Ura +Gal broth (with 4 mM sulfate and varying selenate concentrations) were inoculated to a starting OD_{600} of 0.1 with each yeast strain. Each of the four yeast lines were inoculated in 100 mL aliquots of SD -Ura +Gal broth containing 0 µM, 500 µM, and 5 mM of selenate. These were grown at 30°C in a shaking incubator set to 200 rpm, and the OD_{600} was measured at various time points between 10 and 85 hours. The growth curve assay was conducted three times.

Growth curve assay results were compared using the percentage of baseline growth. That is, OD_{600} readings at each time point in 0 mM selenate for the four yeast strains were used as the controls for their respective strains grown in 500 μM or 5 mM selenate. This was accomplished by dividing the OD reading of the Se-added culture by the OD reading of the Se-absent culture.

2.3.8 Selenate-Sulfate Uptake Assays of Transformed Yeast

Single colonies of each yeast transformant were streaked onto fresh SD -Ura +Dex plates for selection of transformed colonies. These were grown at 30°C for 48 hours. At that time, single colonies of each yeast transformant were used to inoculate 5 mL volumes of SD -Ura +Dex broth in 15 mL culture tubes. These were grown at 30°C, shaking at 200 rpm, ventilated for oxygenation, for 40 hours. At this time, the OD_{600} of each culture was measured. This was used to calculate the appropriate volume of each culture to use to inoculate fresh 100 mL volumes of SD -Ura +Dex broth to an OD_{600} of 0.02. Total volume was determined by estimating a requirement of 50 mL of SD-Ura broth per experimental sample. 100 mL volumes of inoculated broth were incubated in 250 mL baffled flasks, foam-stoppered, shaking at 200 rpm, at 30°C for 36 hours.

At this time, the OD_{600} of each culture was again measured. The experiment proceeded if an OD_{600} above 0.5 had been reached (0.4 was technically the minimum OD for a sufficient quantity of yeast cells). Cells were centrifuged for 5 minutes at 2,200 g. The supernatant was removed, and cells were resuspended in 5 mL SD -Ura +Gal +Raf (1% raffinose). This step was repeated once, and cells of the same line were combined together in 20 mL total volume. Based on the OD_{600}, an appropriate inoculation volume of each cell line was calculated to achieve 75 mL at an OD_{600} of 0.4 in fresh SD -Ura +Gal +Raf. 250 mL baffled flasks were then filled with the calculated volumes, assuming 2 flasks for every 3 samples (each sample needing 50 mL, and

each flask holding 75 mL). These were closed with foam stoppers and grown at 30°C, shaking at 200 rpm, for 12 hours.

After 12 hours, the OD_{600} of each culture was again measured. Cells were centrifuged for 5 minutes at 2,200 g. The supernatant was removed, and cells were resuspended in 5 mL of freshly prepared 25 mM sodium phosphate buffer, pH 6.0. This step was repeated once, and cells of the same line were combined together up to 20 mL total volume. Based on the OD_{600}, additional sodium phosphate buffer was added to bring each cell line to an OD_{600} of 2.0.

Next, baffled flasks were filled to 40 mL with a solution of 25 mM sodium phosphate buffer carrying appropriate concentration of sulfate and selenate. The sulfate, selenate, and sodium phosphate were each drawn from fresh 100 mM stocks. Then, 10 mL of the appropriate cell line was added to achieve 50 mL at an OD_{600} of 0.4, which is above the minimum required to produce a cell pellet sufficient for ICP-MS detection of sulfate and selenate.

As soon as cells were added to the sulfate-selenate buffer solutions, the flasks were foam-stoppered and moved to a room-temperature (24°C) shaker. Flasks were shaken at 150 rpm for exactly 60 minutes. At the end of this period, samples were moved to 50 mL Falcon tubes and centrifuged for 5 min at 2,200 g and 4°C. The supernatant was removed, and the samples were resuspended, with vortexing, in 5 mL of cold 25 mM sodium phosphate buffer. Cells were centrifuged again for 5 min at 2,200 g and 4°C, the supernatant was removed, and cells were then resuspended in 5 mL sterile deionized water. Cells were centrifuged once more, the supernatant was removed, and cells were resuspended in 1 mL sterile deionized water. The cells were then moved to microcentrifuge tubes and centrifuged at 13,200 rpm for 5 minutes. The supernatant was removed, and cell pellets were dried at 50°C for 48 hours in a drying oven, with the tube caps open.

Dried cell pellets were weighed and then transferred to acid-washed glass tubes for nitric acid digestion. Each pellet was floated in 0.5 mL of 70% ultra-pure nitric acid (HNO_3). Each tube was covered with a glass funnel to minimize evaporation during digestion. Tubes were placed into a digestion block, and pellets were digested for 2 hours at 60°C, followed by 6 hours at 130°C. Once the digests cooled, Type 1 water was dispensed from a MilliQ system into each tube, up to 10 mL total volume. These volumes were transferred to 15 mL Falcon tubes. At this point, the digested pellets were in 3.5% nitric acid.

The digests were then analyzed for total Se and S via inductively coupled plasma mass spectrometry (ICP-MS) on an HP Agilent 4500, according to the manufacturer's instructions, using appropriate controls and standards. The detection limit of this machine was approximately 0.1 $\mu g \cdot L^{-1}$ in the digest.

2.3.9 Statistical Analyses

All statistical analyses were run in the computer programming language R (version 3.6.2) with base R functions and additional functions from the *lsmeans* (Lenth, 2016) package. A multiple regression model was built to analyze the one-hour selenate uptake data using the lm() function. This model considered concentration of Se in the yeast as a continuous response, and Se and S supplied to yeast as categorical predictors. Error bars represent one standard error in each direction, as calculated using base R. All sigmoidal curve fits were produced using the SigmaPlot 13 (Systat Software, Inc., San Jose, CA) software package.

2.4 Results

2.4.1 Amino Acid Sequences of *S. pinnata* SULTRs

The amino acid sequences of *S. pinnata* SULTR1;2, SULTR2;1 and SULTR3;5 are shown in alignment with the homologous *A. thaliana* sequences from The Arabidopsis Information Resource (Berardini et al., 2015) in Figures 2.3a, b, and c, respectively. Sequence similarity was the highest between the SULTR1;2 proteins (93.1%), followed by SULTR2;1 (91.5%) and SULTR3;5 (87.5%). All proteins share a similar structure, with an initial cytoplasmic domain, 12 transmembrane domains of a consistent length (21 amino acids), and a final cytoplasmic domain which includes a STAS domain.

The STAS domains of each protein were further examined for sequence differences between homologs. The STAS domains of SULTR2;1 and SULTR3;5 are more divergent between the two species than the STAS domain of SULTR1;2. SULTR2;1 STAS domains of *S. pinnata* and *A. thaliana* demonstrate an 84.9% sequence similarity, and SULTR3;5 STAS domains of the two species demonstrate an 89.7% sequence similarity. However, SULTR1;2 STAS domains of the two species demonstrate a 95.2% sequence similarity. There are 5 nonconservative STAS domain mutations between the *S. pinnata* and *A. thaliana* SULTR2;1 homologs and 2 between the SULTR3;5 homologs (Figure 2.3c).

2.4.2 Selenate Tolerance of Yeast Expressing *S. pinnata* SULTRs

SULTR2;1 and SULTR3;5 from *S. pinnata* were both successfully cloned into a modified (Guignardi, 2017) version of plasmid vector pYES2 and transformed into YPH-500, a yeast strain with intact endogenous sulfate transporters. The yeast lines expressing these proteins are named SpSULTR2;1 and SpSULTR3;5 here. The empty vector was also successfully transformed into this yeast. This line, named pYES2 here, did not express a transgene and functioned as the negative control for all yeast experiments. The previously generated modified pYES2 plasmid with SULTR1;2 from *S. pinnata* (Guignardi, 2017) was also transformed into

YPH-500α. This line, called SpSULTR1;2 here, was also tested in all yeast experiments. Previous work initially indicated preliminary evidence for enhanced selenate specificity of *S. pinnata* SULTR1;2 when expressed in the yeast sulfate transport deficient strain YSD1, but later experiments clearly showed that its selenate specificity was the same as for SULTR1;2 homologues from *S. elata* and *A. thaliana* (Pilon-Smits, unpublished results). SULTR1;2 was tested in the current study to determine whether the same results would be found when expressed in YPH-500.

All yeast strains began to form visible colonies on solid media with 0-3.0 mM selenate after 72 hours (Fig. 2.4a). There were no significant visible differences on the agar plates between any of the lines at this point. As shown in Figure 2.4b, after 120 hours, all four yeast lines began to show inhibited growth at the 10^{-3} dilution level when exposed to 1.5 mM Se. Growth inhibition begins to appear after 120 hours at the OD_{600} level of 1.0 at 2.5 mM Se, and growth remains completely inhibited by 5.0 mM Se. Overall, there were no visible differences in the tolerance of YPH-500 yeast expressing any of the three SULTRs or the yeast with the pYES2 empty vector, whether assessed at 72 hours or 120 hours.

2.4.3 Growth Curves of Yeast Expressing *S. pinnata* SULTRs

The growth curves of each of the four yeast lines in liquid medium are shown in Figure 2.5. Each growth curve was estimated with a sigmoid fit, based on previous research (Richards, 1928; Sun et al., 2010). Each line demonstrated strong growth inhibition when exposed to 5 mM Se. All lines lagged in the exponential growth phase when exposed to 0.5 mM Se as compared to 0 mM Se, although all lines except SULTR3;5 also grew to higher final concentrations in 0.5 mM Se than 0 mM Se. SULTR2;1 (Fig. 2.5c) and SULTR3;5 (Fig. 2.5d) grew to slightly lower final concentrations in 0.5 mM Se than the empty vector pYES2 (Fig. 2.5a).

Figure 2.6 presents a subset of the data in Figure 2.5 for further inspection. Specifically, it presents growth after 85 hours in either 0.5 mM or 5 mM Se as a percentage of the growth achieved for the same line in 0 mM Se after 85 hours. This demonstrates each line was severely inhibited by exposure to 5 mM Se, relative to its own 0 mM Se growth pattern. However, this figure also indicates that the empty vector line grew slightly better than the SULTR-expressing lines, especially SULTR2;1 and SULTR3;5 at the 0.5 mM Se level.

2.4.4 Selenate-Sulfate Uptake of Yeast Expressing *S. pinnata* SULTRs

Results of the one-hour selenate-sulfate uptake assays are presented in Figure 2.7. Figure 2.7a indicates that yeast lines SpSULTR1;2 and SpSULTR2;1 tended to take up more Se than the empty vector line pYES2 when exposed to 1 mM selenate with no competing sulfate. The line SpSULTR3;5 demonstrated a significant reduction in selenate uptake relative to all of the other lines, including the empty vector. In contrast, when yeast lines were exposed to the 10X lower concentration of 0.1 mM selenate (again without competing sulfate), SpSULTR1;2 and SpSULTR2;1 showed a reduction in selenate uptake relative to pYES2, and SpSULTR3;5 took up a similar amount of selenate to pYES2. In the 0.1 mM selenate assay, variance was notably high in both the pYES2 and SpSULTR2;1 lines. When challenged with 5 mM sulfate, selenate uptake fell sharply in all cases. In the 5 mM sulfate and 0.1 mM selenate assay, selenate uptake fell to zero in all lines. In the 5 mM sulfate and 1 mM selenate assay, selenate uptake fell to a level approximately equal to the water-only negative control assay.

Figure 2.7b examines the data from another perspective, using the ratio of selenate to sulfate in the yeast as the response variable; the sulfate data are presented in Figure 2.7c. Figure 2.7b confirms that there is no observed difference in the uptake of selenate relative to sulfate in

SULTR2;1 as compared to SULTR1;2. SULTR3;5 again appears to take up more selenate relative to sulfate in the 0.1 mM sulfate treatment than the 1.0 mM sulfate treatment.

2.5 Discussion

The goals of this project were to determine whether the putative sulfate / selenate transporters SpSULTR2;1 and SpSULTR3;5 from Se hyperaccumulator *S. pinnata* are able to transport selenate, and whether either displays increased preference for the uptake of selenate over sulfate, relative to the earlier characterized SpSULTR1;2. Although the comparative sequence analyses of the *S. pinnata* and *A. thaliana* SULTR2;1 and SULTR3;5 sequences revealed differences which could potentially translate to altered functionality in the *S. pinnata* homologs, we found no evidence that either SpSULTR2;1 or SpSULTR3;5 preferentially transported selenate over sulfate relative to SpSULTR1;2. Furthermore, we found no clear, consistent evidence to support the assertion that SpSULTR2;1 and SpSULTR3;5 are capable of transporting selenate.

Based on the dot blot immunoassay, the SpSULTR proteins were expressed in the yeast. Perhaps the combined activity of the endogenous sulfate transporters in the YPH500 yeast strain overshadowed the activity of the introduced plant transporters. Past studies have used the YSD1 mutant *S. cerevisiae* strain lacking the endogenous SUL1 sulfate transporter, because the effects of subsequently introduced SULTR transgenes can be more easily assessed without a competing sulfate transporter (El Kassis et al., 2007; Guignardi, 2017). However, this strain has proven difficult to grow under low-S conditions (Guignardi, 2017), which were required for our uptake study. Rather than experiment with stressed cultures of YSD1, we elected to experiment with robust cultures of YPH500, accepting the trade-off that the SULTR-transformed yeast would likely show a smaller magnitude increase in selenate uptake than if YSD1 had been used.

The selenate tolerance assay on solid medium did not yield significant evidence of selenate transport by the *Stanleya* SULTRs. Yeast strains SpSULTR1;2, SpSULTR2;1, and SpSULTR3;5 all demonstrated approximately the same level of selenate resistance as compared to yeast expressing the empty vector pYES2. All yeast lines began to show inhibited growth on solid medium at the 10^{-3} dilution level when exposed to 1.5 mM Se, and at the undiluted (OD_{600} = 1.0) level when exposed to 2.5 mM Se. Furthermore, growth of all lines was completely inhibited by 5.0 mM Se (Figure 2.4). Overall, there was no reduction in tolerance in the SULTR-expressing lines to indicate that these yeast cells were taking up more selenate from the solid medium and suffering relatively reduced growth as a result.

Similarly, the growth curve assay in liquid medium did not indicate poorer growth in the SULTR-expressing lines relative to the pYES2-only line when exposed to selenate. All yeast showed growth inhibition when exposed to 5 mM Se (Figure 2.5). When exposed to 0.5 mM Se, all lines showed similar growth except for SpSULTR 3;5, which had a delayed growth curve and lower maximum concentration than the other lines. However, this result was found in both the Se-negative and 0.5 mM Se treatments, so it could not be attributed to an increase in selenate uptake. Instead, this may indicate that the expression of SULTR3;5 had some toxic effect for the yeast. However, when growth in Se-positive treatments (both 0.5 mM Se and 5 mM Se) was analyzed as a percentage of baseline (Se-negative) growth (Figure 2.6), the SULTR-expressing lines all demonstrated slightly lower relative growth than the pYES2 empty vector. This could indicate that the SULTR-expressing lines were taking up more Se than the pYES2 line, causing a marginally more pronounced growth inhibition. In addition, it cannot be ruled out that the SULTR-expressing yeast lines would have shown evidence of increased selenate uptake at some intermediate selenate concentration.

The one-hour Se uptake assays yielded conflicting evidence regarding the ability of the SULTRs to transport selenate. As shown in Figure 2.7a, SpSULTR1;2 and SpSULTR2;1 yeast lines tended to take up more Se than the pYES2 line when exposed to 1 mM selenate, but the SpSULTR3;5 yeast line took up significantly less Se than the pYES2 line. Furthermore, when the Se dose was 0.1 mM (10X lower), the results were significantly different. When exposed to this low dose, SpSULTR1;2 and SpSULTR2;1 took up very little Se, and pYES2 and SpSULTR3;5 lines took up more. Another surprising result was that, at both the 0.1 mM Se and 1 mM Se levels, one or more SpSULTR-expressing yeast lines took up less Se than the pYES2 empty vector line. This result is unexpected because of the prevailing theory that plant SULTRs have at least some selenate transport capacity (White, 2018), which has experimental evidence to support it in the case of SULTR1;2 (Shibagaki et al., 2002). As discussed in the next paragraph, these patterns may be explained in multiple ways—each of which should be explored in future experiments.

First, it is possible—but unlikely—that SpSULTR2;1 and SpSULTR3;5 have no selenate transport capacity. Despite the fact that neither SULTR significantly increased Se uptake over the negative control at any sulfate-selenate treatment level (Figure 2.7a), the similarity of the chemical structure of the sulfate and selenate ions makes them less differentiable to SULTRs, especially low-affinity sulfate transporters like SULTR2;1 and SULTR3;5 (Kataoka et al., 2004; Takahashi et al., 2000). Furthermore, Figure 2.7a indicates a large amount of variance in the uptake results for pYES2 and SULTR2;1 when exposed to 0.1 mM selenate. Future studies should consider using a larger sample size to enhance the detection of differences between the transporters. It is also possible that the expression level of the encoded SULTRs varied. Unfortunately, expression levels could not be determined because traditional Western Blot

methods failed, possibly because the transporter proteins were not efficiently extracted by the sample buffer. This led us to rely on the total protein nitrocellulose blot for a positive-negative indication of expression. The total protein blot, shown in Figure 2.2, did confirm expression of all three SULTRs, but was not quantifiable. Expression levels may be affected by factors such as the half-life of the transcribed mRNA (Brown et al., 1988) and the half-life of the encoded protein (Dice, 1987). Furthermore, it can be difficult to achieve high expression levels of heterologous membrane proteins in yeast if the proteins have a large number of membrane-spanning domains—especially if there are 7 or more such domains (M. A. White et al., 2007). Each SULTR protein in this study has 12 membrane-spanning domains. This may have led to detectable but low expression of the SULTRs, allowing the endogenous SUL1 transporter to overshadow their effects. Additionally, expression of an exogenous membrane protein may have induced unanticipated physiological changes in the yeast (Romanos et al., 1992). For example, *S. cerevisiae* expression of the membrane-localized proteins influenza hemagglutinin (Jabbar et al., 1985), polyoma virus middle-T antigen (Belsham et al., 1986), and *E. coli* OmpA protein (Janowicz et al., 1982), all reduce the growth rate of the host. This potentially toxic effect has been hypothesized to be due to nonspecific insertion into the yeast membrane (Romanos et al., 1992). This disruption of normal yeast membrane structure could affect the growth of the SULTR-expressing yeast strains, leading to the seemingly contradictory results in this study.

From these results, we cannot definitively conclude whether SpSULTR2;1 or SpSULTR3;5 possess Se transport capacity. The challenging nature of these results lead us to multiple recommendations for future studies of SULTR Se transport functionality in yeast model systems. First, this experiment should be repeated with more samples per treatment group to reduce variability. Second, a sensitive and highly specific detection method for the quantification

of SULTR protein expression in yeast must be developed, to standardize the uptake results relative to the magnitude of expression. Finally, more Se and S concentrations should be tested, in order to find uptake patterns that may have been invisible in the present study. For example, important changes in the uptake capacity of one or more SULTR-expressing yeast lines may have occurred between 0.1 mM and 1.0 mM Se. Alternatively, S concentrations between 0 and 5.0 mM could have produced unforeseen effects. For instance, SpSULTR1;2 and SpSULTR2;1 yeast lines were able to take up more Se than the empty vector pYES2 line when treated with 1 mM Se, but Se uptake across all three lines was similarly repressed when exposed to 1 mM Se with 5 mM S. However, an intermediate S level—for example, 1 mM S—may have shown greater repression of Se uptake in the pYES2 line than in the SULTR-expressing lines. From these suggested additional experiments, more can be learned about the S and Se transport capacities of the *S. pinnata* SULTRs.

2.6 Figures

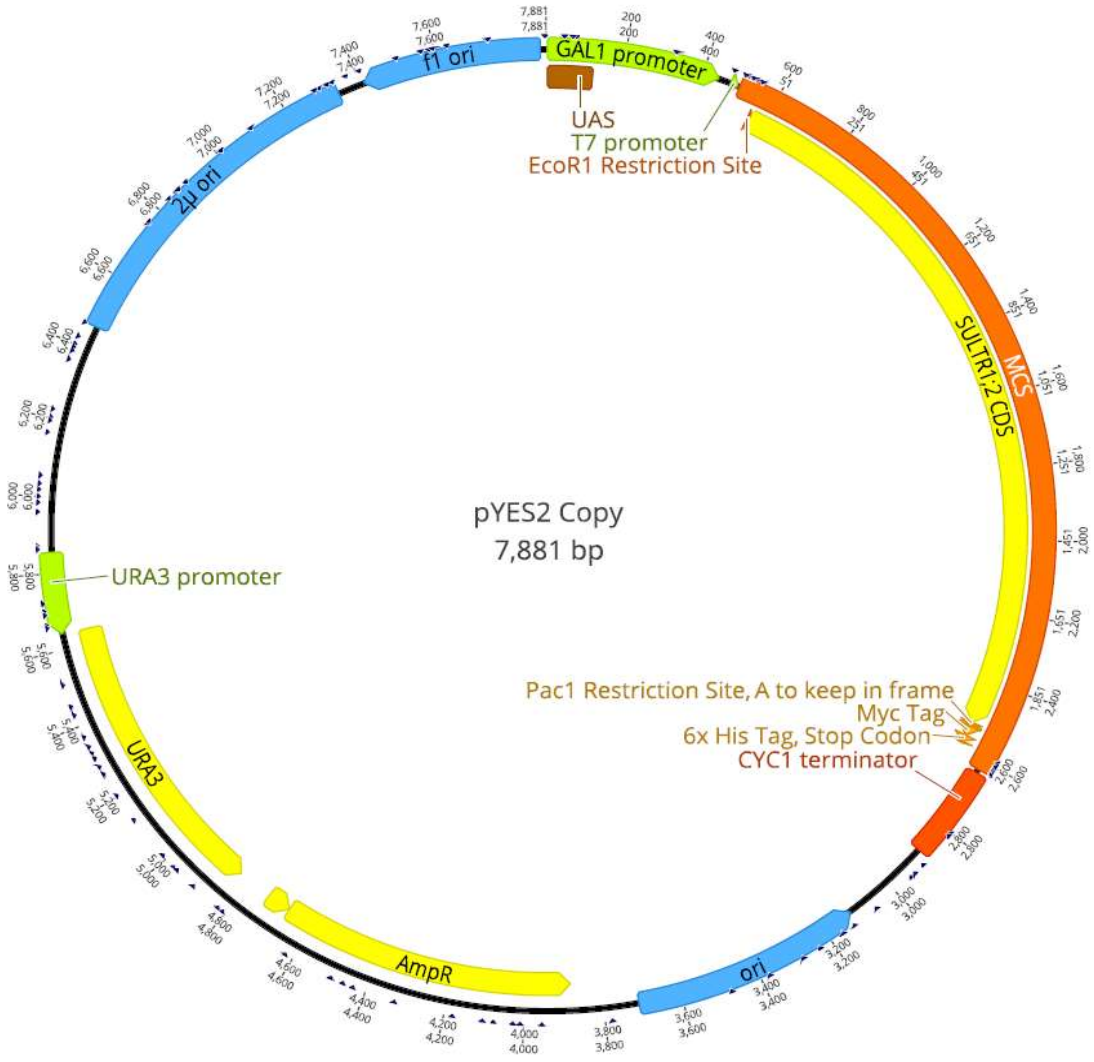

Figure 2.1. Diagram of the pYES2 plasmid, constructed in Geneious from ThermoFisher pYES2 sequence data and annotations. Plasmid modified with the insertion of the SULTR1;2 coding sequence with 3' Myc and His tags attached.

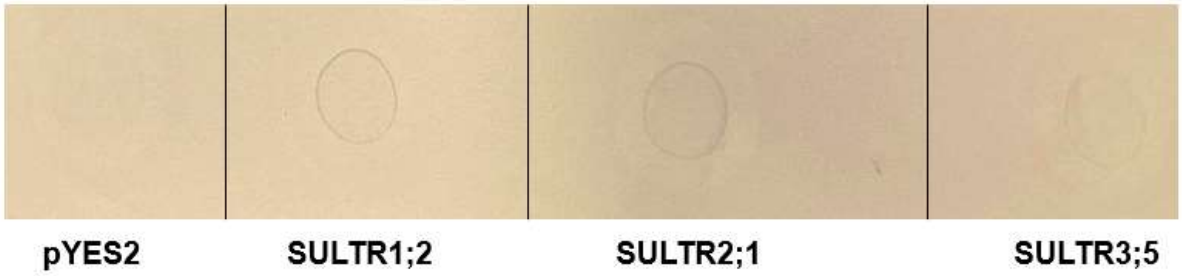

Figure 2.2. Nitrocellulose blot of SULTR proteins expressed by transformed YPH500-α yeast. From left to right: negative control yeast transformed with pYES2 empty vector, yeast expressing SpSULTR1;2, yeast expressing SpSULTR2;1, and yeast expressing SpSULTR3;5. 5 µg of total protein from each yeast transformant was pipetted onto nitrocellulose and incubated with anti-Myc mouse primary antibody (Thermofisher), followed by incubation with anti-mouse horseradish peroxidase secondary antibody. Nitrocellulose was then exposed to a 10 mL solution of NBT-BCIP for 5 minutes, rinsed in deionized water, and air dried.

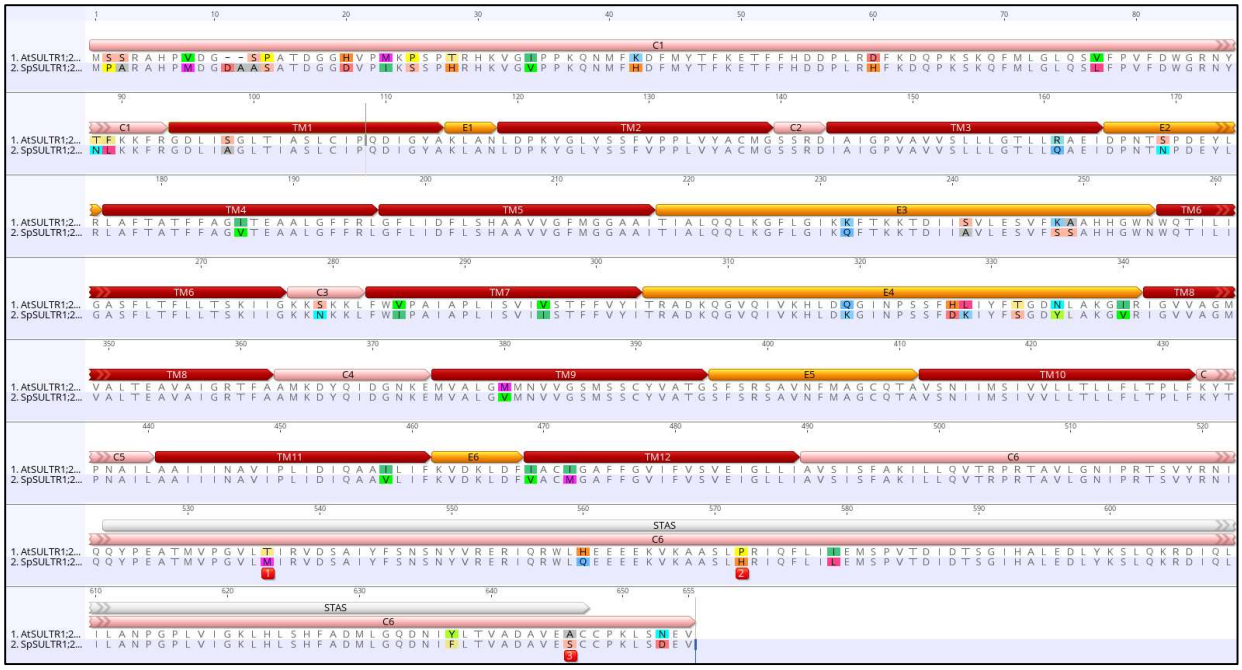

Figure 2.3a. Amino acid sequence of SULTR1;2 from *A. thaliana* (top rows) versus *S. pinnata* (bottom rows). Cytoplasmic domains ("C#"), transmembrane domains ("TM#"), extracellular domains ("E#"), and the STAS domain ("STAS") are labeled. Nonconservative amino acid substitutions in the STAS domain are underscored with a numerical value, where number 1 corresponds to the first nonconservative substitution counting from the N-terminus to the C-terminus of the STAS domain.

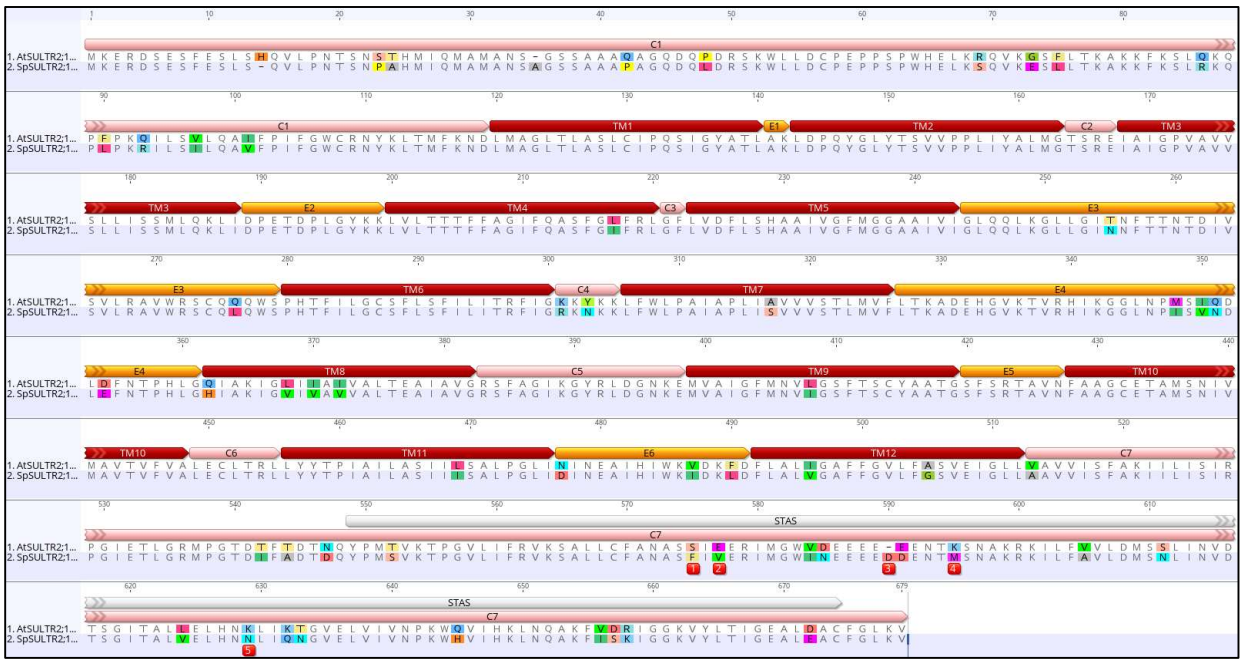

Figure 2.3b. Amino acid sequence of SULTR2;1 from *S. pinnata* (bottom rows) versus *A. thaliana* (top rows). Cytoplasmic domains ("C#"), transmembrane domains ("TM#"), extracellular domains ("E#"), and the STAS domain ("STAS") are labeled. Nonconservative amino acid substitutions in the STAS domain are underscored with a numerical value, where number 1 corresponds to the first nonconservative substitution counting from the N-terminus to the C-terminus of the STAS domain.

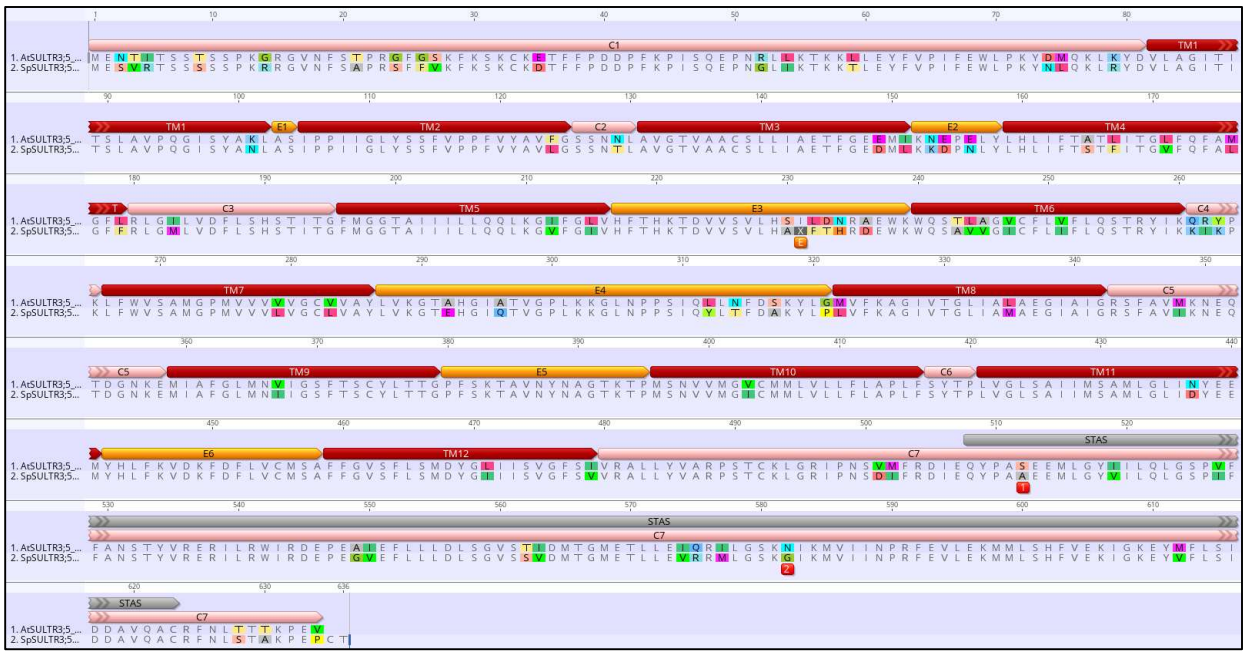

Figure 2.3c. Amino acid sequence of SULTR3;5 from *S. pinnata* (bottom rows) versus *A. thaliana* (top rows). Cytoplasmic domains ("C#"), transmembrane domains ("TM#"), extracellular domains ("E#"), and the STAS domain ("STAS") are labeled. Nonconservative amino acid substitutions in the STAS domain are underscored with a numerical value, where number 1 corresponds to the first nonconservative substitution counting from the N-terminus to the C-terminus of the STAS domain.

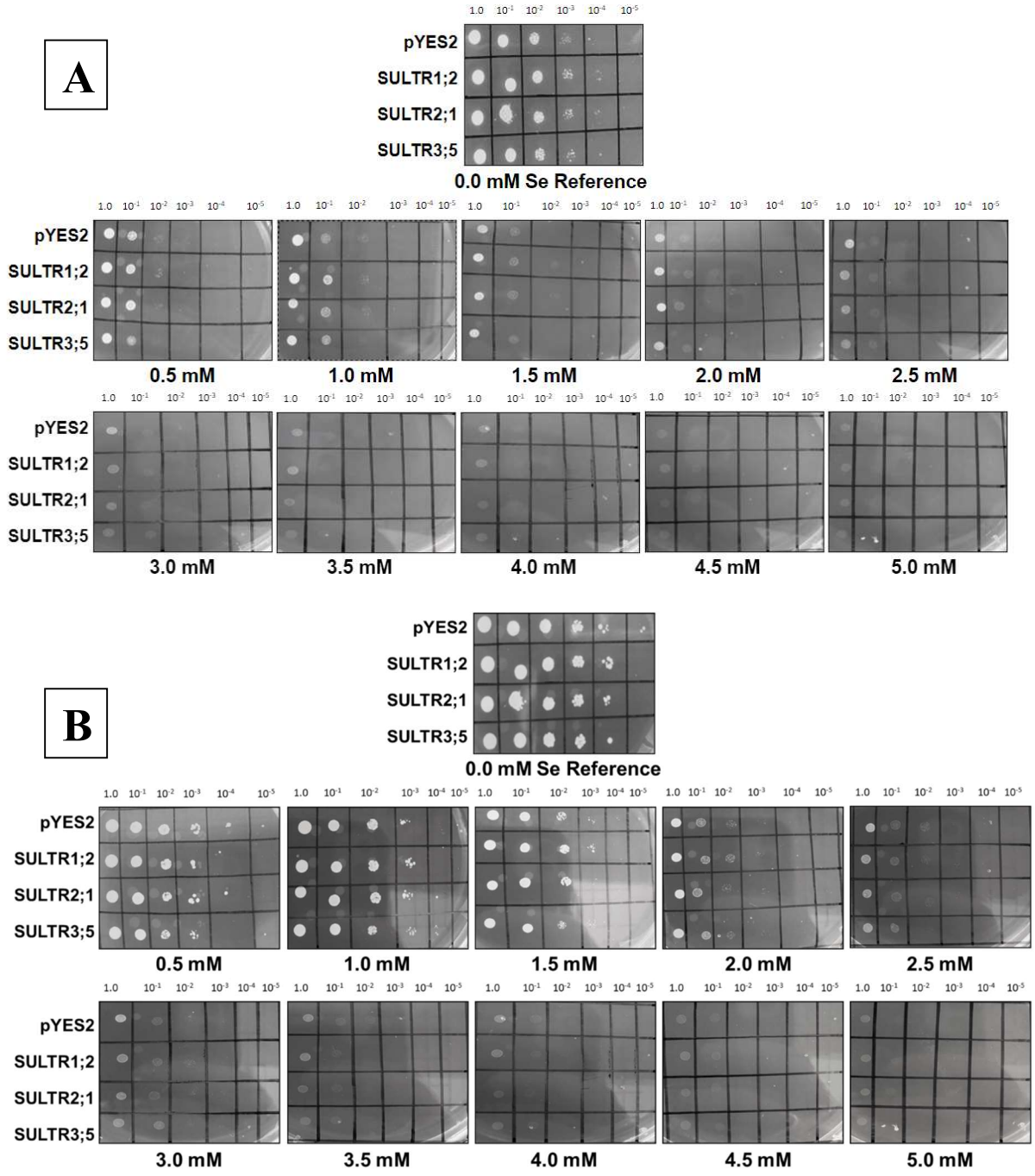

Figure 2.4. Growth of dilution series of indicated (left) transformed YPH500-α yeast lines after (**A**) 72 hours and (**B**) 120 hours on SD -Ura +Gal agar with indicated selenate concentrations ranging from 0.0-5.0 mM. Lines are labeled at left of each row. Se concentration is labeled below each image. OD_{600} of the dilution is labeled above each dot column.

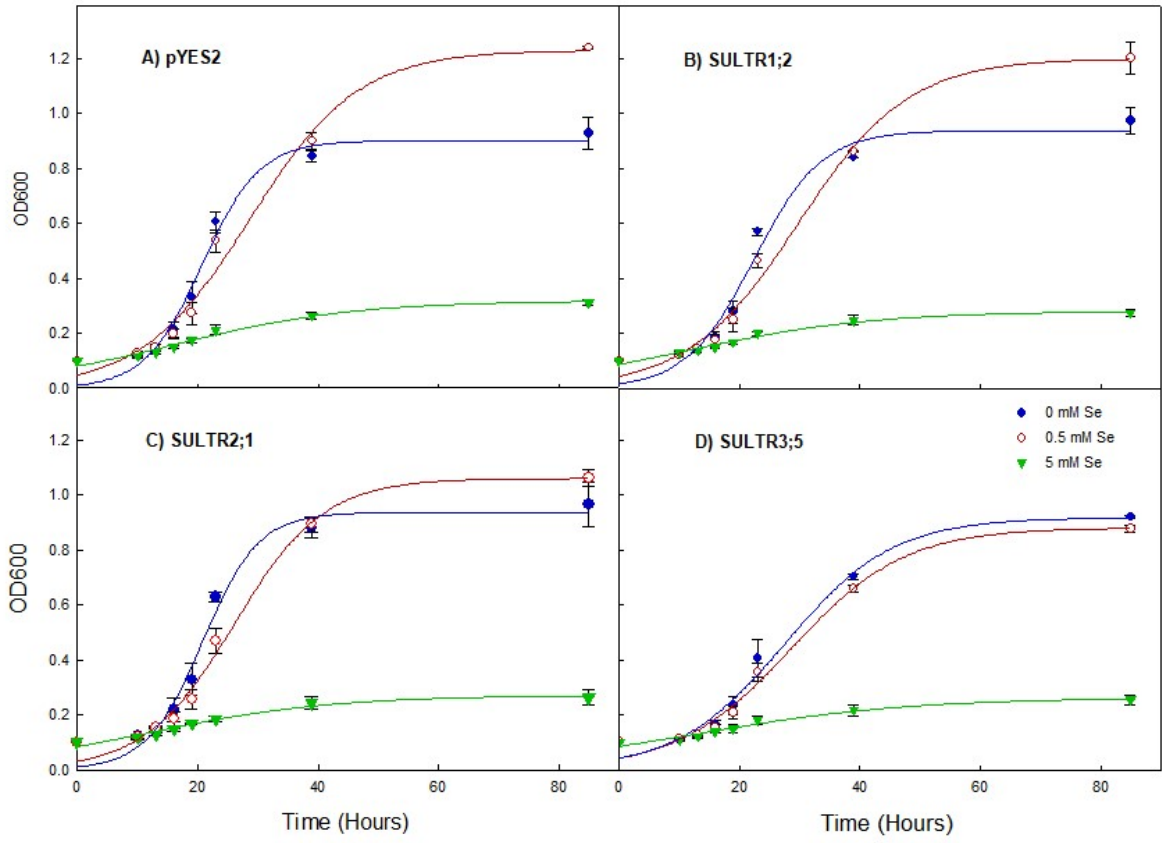

Figure 2.5. Growth curves of YPH500-α expressing SpSULTR1;2, 2;1, or 3;5, or transformed with pYES2 empty vector, in synthetic defined liquid media. Y axis indicates growth as measured by OD_{600}, and X axis indicates time in hours. Media supplemented with 0 mM Se (blue lines), 0.5 mM Se (red lines), or 5 mM Se (green lines). Each growth curve experiment was run once, with three samples per experimental group.

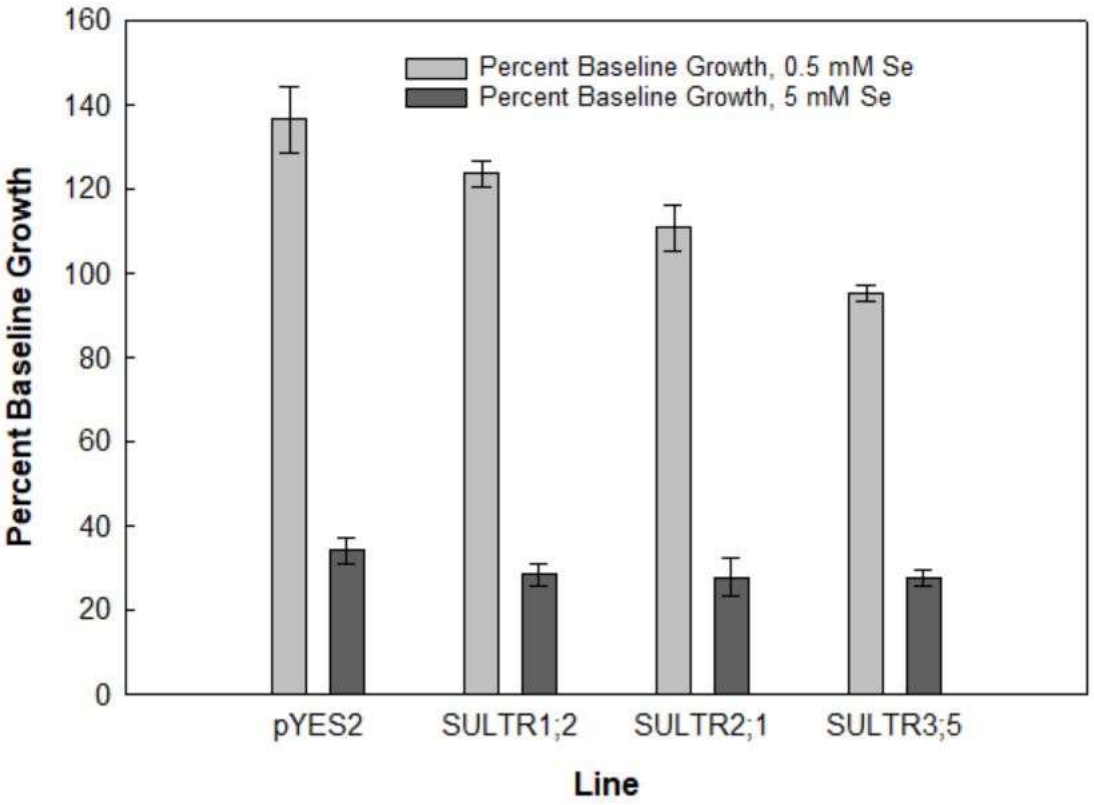

Figure 2.6. Percent of baseline (0 mM Se) growth of yeast lines after 85 hours. This figure is produced using the growth curve data from Figure 2.5.

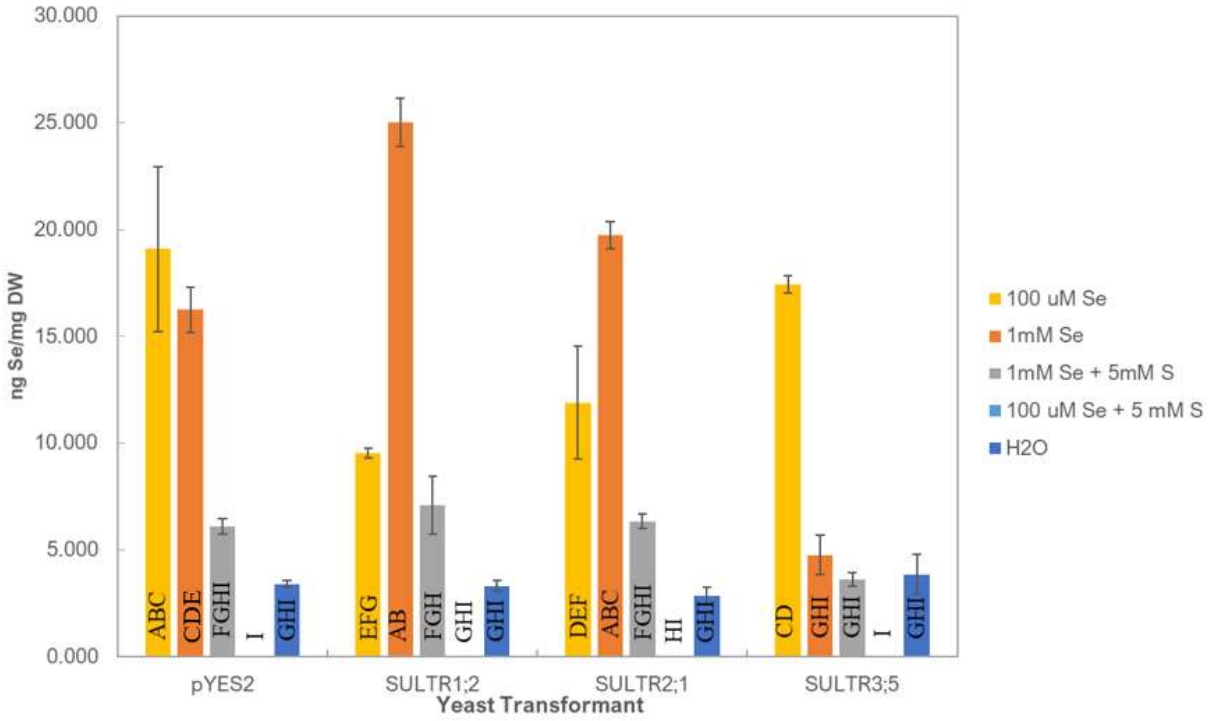

Figure 2.7a. ICP measurements of mean (n = 3) nanograms of Se per milligram of dry weight in yeast expressing SULTRs or empty vector after 1 hour uptake of various concentrations of selenate and sulfate (see legend at right). Letters at the base of each bar indicate significance groups ($\alpha = 0.05$), as calculated by ANOVA with Tukey-Kramer adjustment. Error bars are +/- one standard error.

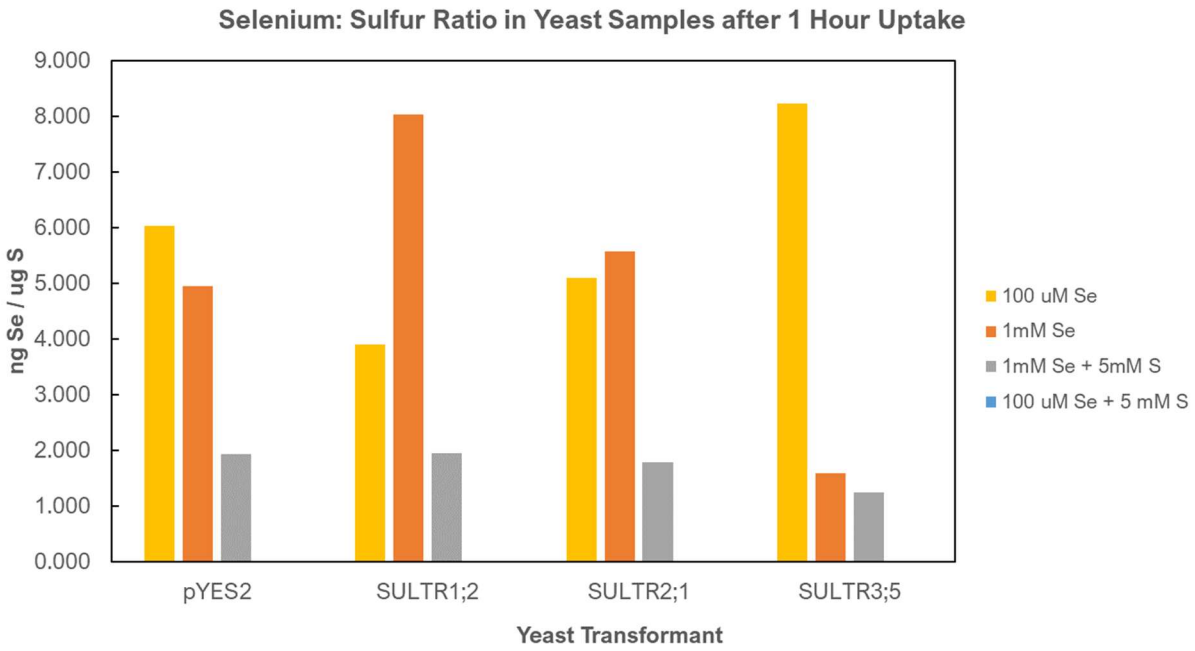

Figure 2.7b. The ratio of nanograms of Se per microgram of S in yeast expressing SULTRs or empty vector after 1 hour uptake of various concentrations of selenate and sulfate (see legend at right). Error bars are not included because this ratio is the division of two measured variables, and the compounded error is too large to test for significant differences.

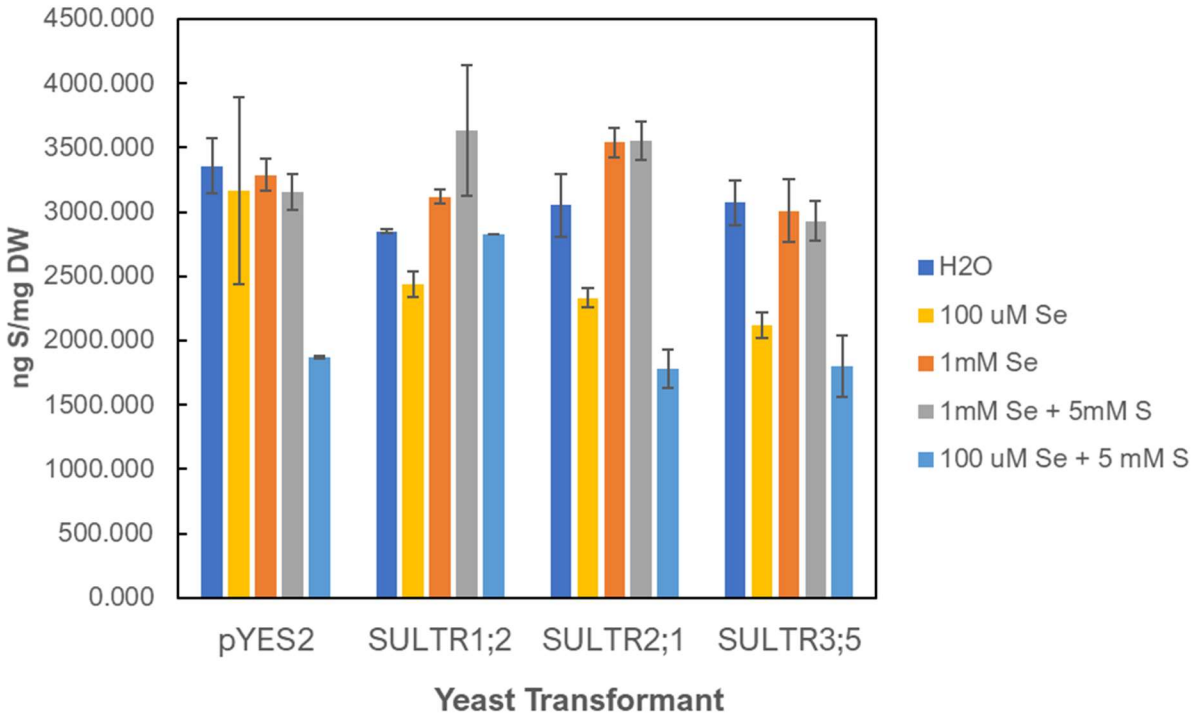

Figure 2.7c. ICP measurement of nanograms S per milligram dry weight of yeast samples after 1 hour uptake assays (means +/- one standard error).

LITERATURE CITED

Anderson, J.W., 1993. Selenium interactions in sulfur metabolism, in: De Kok, L.J., Stulen, I., Rennenberg, H., Brunold, C., Rauser, W.E. (Eds.), Sulfur Nutrition and Assimilation in Higher Plants: Regulatory Agricultural and Environmental Aspects. SPB Academic Publishing, The Hague, pp. 49–60.

Barberon, M., Berthomieu, P., Clairotte, M., Shibagaki, N., Davidian, J.C., Gosti, F., 2008. Unequal functional redundancy between the two Arabidopsis thaliana high-affinity sulphate transporters SULTR1;1 and SULTR1;2. New Phytol. 180, 608–619. https://doi.org/10.1111/j.1469-8137.2008.02604.x

Belsham, G.J., Barker, D.G., Smith, A.E., 1986. Expression of polyoma virus middle-T antigen in Saccharomyces cerevisiae. Eur. J. Biochem. 156, 413–421. https://doi.org/10.1111/j.1432-1033.1986.tb09598.x

Berardini, T.Z., Reiser, L., Li, D., Mezheritsky, Y., Muller, R., Strait, E., Huala, E., 2015. The arabidopsis information resource: Making and mining the "gold standard" annotated reference plant genome. Genesis 53, 474–485. https://doi.org/10.1002/dvg.22877

Brown, A.J.P., Purvis, I.J., Santiago, T.C., Bettauy, A.J.E., Loughh, L., Moore, J., 1988. Messenger RNA degradation in Saccharomyces cerevisiae. Gene 72, 151–160. https://doi.org/10.1016/0378-1119(88)90137-0

Cabannes, E., Buchner, P., Broadley, M.R., Hawkesford, M.J., 2011. A Comparison of Sulfate and Selenium Accumulation in Relation to the Expression of Sulfate Transporter Genes in Astragalus Species. Plant Physiol. 157, 2227–2239. https://doi.org/10.1104/pp.111.183897

Cappa, J.J., Cappa, P.J., El Mehdawi, A.F., McAleer, J.M., Simmons, M.P., Pilon-Smits, E.A.H., 2014. Characterization of selenium and sulfur accumulation across the genus Stanleya (Brassicaceae): A field survey and common-garden experiment. Am. J. Bot. 101, 830–839. https://doi.org/10.3732/ajb.1400041

Cao, M.J., Wang, Z., Wirtz, M., Hell, R., Oliver, D.J., Xiang, C.-B., 2013. SULTR3;1 is a chloroplast-localized sulfate transporter in Arabidopsis thaliana. Plant J. 73, 607–616. https://doi.org/10.1111/tpj.12059

Dice, J.F., 1987. Molecular determinants of protein half-lives in eukaryotic cells. FASEB J. 1, 349–357. https://doi.org/10.1096/fasebj.1.5.2824267

Gietz, R.D., Schiestl, R.H., 2007. High-efficiency yeast transformation using the LiAc / SS carrier DNA / PEG method. Nat. Protoc. 2, 31–35. https://doi.org/10.1038/nprot.2007.13

Guignardi, Z.S., 2017. Studies on selenium hyperaccumulator Stanleya pinnata and nonaccumulator Stanleya elata (Brassicaceae): Functional characterization of selenate

transporter SULTR1;2 in yeast and developent of a micropropagation protocol. Colorado State University.

Jabbar, M.A., Sivasubramanian, N., Nayak, D.P., 1985. Influenza viral (A/WSN/33) hemagglutinin is expressed and glycosylated in the yeast Saccharomyces cerevisiae. Proc. Natl. Acad. Sci. U. S. A. 82, 2019–2023. https://doi.org/10.1073/pnas.82.7.2019

Janowicz, Z.A., Henning, U., Hollenberg, C.P., 1982. Synthesis of Escherichia coli outer membrane OmpA protein in yeasts. Gene 20, 347–358. https://doi.org/10.1016/0378-1119(82)90203-7

Kataoka, T., Hayashi, N., Yamaya, T., Takahashi, H., 2004. Root-to-Shoot Transport of Sulfate in Arabidopsis. Evidence for the Role of SULTR3;5 as a Component of Low-Affinity Sulfate Transport System in the Root Vasculature. Plant Physiol. 136, 4198–4204. https://doi.org/10.1104/pp.104.045625

Lenth, R. V, 2016. Least-Squares Means: The R Package lsmeans. J. Stat. Softw. 69, 1–33. https://doi.org/10.18637/jss.v069.i01

Richards, O.W., 1928. Potentially unlimited multiplication of yeast with constant environment, and the limiting of growth by changing environment. Gen. Physiol. 525–538.

Romanos, M.A., Scorer, C.A., Clare, J.J., 1992. Foreign Gene Expression in Yeast: A Review. Yeast 8, 1–66.

Rouached, H., Berthomieu, P., El Kassis, E., Cathala, N., Catherinot, V., Labesse, G., Davidian, J.C., Fourcroy, P., 2005. Structural and functional analysis of the C-terminal STAS (sulfate transporter and anti-sigma antagonist) domain of the Arabidopsis thaliana sulfate transporter SULTR1.2. J. Biol. Chem. 280, 15976–15983. https://doi.org/10.1074/jbc.M501635200

Shibagaki, N., Grossman, A.R., 2006. The role of the STAS domain in the function and biogenesis of a sulfate transporter as probed by random mutagenesis. J. Biol. Chem. 281, 22964–22973. https://doi.org/10.1074/jbc.M603462200

Shibagaki, N., Grossman, A.R., 2004. Probing the function of STAS domains of the Arabidopsis sulfate transporters. J. Biol. Chem. 279, 30791–30799. https://doi.org/10.1074/jbc.M403248200

Sikorski, R.S., Hieter, P., 1989. A System of Shuttle Vectors and Yeast Host Strains Designed for Efficient Manipulation of DNA in Saccharomyces ceratisiae. Genetics 122, 19–27.

Sun, J., Stowers, C.C., Boczko, E.M., Li, D., 2010. Measurement of the volume growth rate of single budding yeast with the MOSFET-based microfluidic Coulter counter. Lab Chip 10, 2986–2993. https://doi.org/10.1039/c005029f

Takahashi, H., Watanabe-Takahashi, A., Smith, F.W., Blake-Kalff, M., Hawkesford, M.J., Saito, K., 2000. The roles of three functional sulphate transporters involved in uptake and translocation of sulphate in Arabidopsis thaliana. Plant J. 23, 171–182. https://doi.org/10.1046/j.1365-313X.2000.00768.x

Taylor, R.G., Walker, D.C., Mclnnes, R.R., 1993. E.coli host strains significantly affect the quality of small scale plasmid DNA preparations used for sequencing. Nucleic Acids Res. 21, 1677–1678. https://doi.org/10.1093/nar/21.7.1677

Van Hoewyk, D., 2013. A tale of two toxicities: malformed selenoproteins and oxidative stress both contribute to selenium stress in plants. Ann. Bot. 112, 965–972. https://doi.org/10.1093/aob/mct163

Wang, J., Cappa, J.J., Harris, J.P., Edger, P.P., Zhou, W., Pires, J.C., Adair, M., Unruh, S.A., Simmons, M.P., Schiavon, M., Pilon-Smits, E.A.H., 2018. Transcriptome-wide comparison of selenium hyperaccumulator and nonaccumulator Stanleya species provides new insight into key processes mediating the hyperaccumulation syndrome. Plant Biotechnol. J. 16, 1582–1594. https://doi.org/10.1111/pbi.12897

White, M.A., Clark, K.M., Grayhack, E.J., Dumont, M.E., 2007. Characteristics Affecting Expression and Solubilization of Yeast Membrane Proteins. J. Mol. Biol. 365, 621–636. https://doi.org/10.1016/j.jmb.2006.10.004

White, P.J., Bowen, H.C., Marshall, B., Broadley, M.R., 2007. Extraordinarily high leaf selenium to sulfur ratios define 'Se-accumulator' plants. Ann. Bot. 100, 111–118. https://doi.org/10.1093/aob/mcm084

White, P.J., 2018. Selenium metabolism in plants. Biochim. Biophys. Acta - Gen. Subj. 1862, 2333–2342. https://doi.org/10.1016/j.bbagen.2018.05.006

Zhang, Y., Gladyshev, V.N., 2009. Comparative genomics of trace elements: Emerging dynamic view of trace element utilization and function. Chem. Rev. 109, 4828–4861. https://doi.org/10.1021/cr800557s

APPENDIX 1

Table A1.1 All primers used in Chapter 2 experiments.

Name	Purpose	Direction	Features	Sequence
pYES2_Fwd	Sequence from pYES2 T7 promoter into gene insert	Forward	NA	5' TAATACGACT CACTATAGGG 3'
Sp2;1_Insert_Fwd	Amplify SpSULTR2;1 coding sequence for plasmid insertion	Forward	5'-End: four random bases, then EcoRI Site	5' GAGCGAATTCATGAAA GAACGAGATTCAGAGAG 3'
Sp2;1_Insert_Rev	Amplify SpSULTR2;1 coding sequence for plasmid insertion	Reverse	5'-End: four random bases, then PacI Site	5' GAGCTTAATTAAAACTT TTAATCCAAAGCAAGC 3'
Sp2;1_Start_Fwd	SpSULTR2;1 Sequencing	Forward	NA	5' GGTAATCTTC CACGCAACCG 3'
Sp2;1_1Qtr_Fwd	SpSULTR2;1 Sequencing	Forward	NA	5' GGCCTATATA CGAGCGTGG 3'
Sp2;1_1Qtr_Rev	SpSULTR2;1 Sequencing	Reverse	NA	5' TCTCCCGAGC GTTTCAATCC 3'
Sp2;1_Half_Fwd	SpSULTR2;1 Sequencing	Forward	NA	5' GATTTCCGTCT TAGTGTCAACG 3'
Sp2;1_Half_Rev	SpSULTR2;1 Sequencing	Reverse	NA	5' CACCATTAACGT TGACACTAAGAC 3'
Sp2;1_3Qtr_Fwd	SpSULTR2;1 Sequencing	Forward	NA	5' GGTTCTGTCGA GATCGGACTC 3'
Sp2;1_3Qtr_Rev	SpSULTR2;1 Sequencing	Reverse	NA	5' TCTCCCGAGC GTTTCAATCC 3'
Sp2;1_End_Rev	SpSULTR2;1 Sequencing	Reverse	NA	5' TCACATGCAACAA TACGTAAAACAC 3'
Sp3;5_Insert_Fwd	Amplify SpSULTR3;5 coding sequence for plasmid insertion	Forward	5'-End: four random bases, then EcoRI Site	5' GAGCGAATTCATGGAG AGTGTTAGAACAAGCTC 3'
Sp3;5_Insert_Rev	Amplify SpSULTR3;5 coding sequence for plasmid insertion	Reverse	5'-End: four random bases, then PacI Site	5' GAGCTTAATTAAAGTAC AGGGTTCGGGTTTGGC 3'
Sp3;5_Start_Fwd	SpSULTR3;5 Sequencing	Forward	NA	5' TTGCTTGCTT GTTGTGGGTG 3'
Sp3;5_1Qtr_Fwd	SpSULTR3;5 Sequencing	Forward	NA	5' GCCGTTCCTC AGGGTATCAG 3'
Sp3;5_1Qtr_Rev	SpSULTR3;5 Sequencing	Reverse	NA	5' CACCGCGAGA GTGTTCGAAC 3'
Sp3;5_Half_Fwd	SpSULTR3;5 Sequencing	Forward	NA	5' CCCTCCTTCTATT CAATATTTGACC 3'
Sp3;5_Half_Rev	SpSULTR3;5 Sequencing	Reverse	NA	5' ACCAACGGTA GATACTTGGCA 3'
Sp3;5_3Qtr_Fwd	SpSULTR3;5 Sequencing	Forward	NA	5' GCCCTCGACTT GTAAATTGGG 3'
Sp3;5_3Qtr_Rev	SpSULTR3;5 Sequencing	Reverse	NA	5' GCGGCAGGGTA CTGTTCTATG 3'
Sp3;5_End_Rev	SpSULTR3;5 Sequencing	Reverse	NA	5' ACCTTCCACTAAT AACTAAGTACAGG 3'

Table A1.2. All PCR protocols used in Chapter 2 experiments.

<table>
<tr><th>Name and Purpose</th><th>Reagents</th><th>Steps</th></tr>
<tr><td>SpSULTR2;1 Amplification</td><td>
<table>
<tr><th>Name and Concentration</th><th>µL</th><th>Final Concentration</th></tr>
<tr><td>PCR grade H20, NA</td><td>13.5</td><td>NA</td></tr>
<tr><td>5X Phusion HF Buffer</td><td>5</td><td>1X</td></tr>
<tr><td>dNTP Mix, 2 mM</td><td>2.5</td><td>200 µM</td></tr>
<tr><td>Forward Primer, 10 µM</td><td>1.25</td><td>0.5 µM</td></tr>
<tr><td>Reverse Primer, 10 µM</td><td>1.25</td><td>0.5 µM</td></tr>
<tr><td>Phusion DNA Polymerase</td><td>0.5</td><td>1.0 units/25uL PCR</td></tr>
<tr><td>Template, 25 ng/µL</td><td>1</td><td>1 ng/µL</td></tr>
</table>
</td><td>
<table>
<tr><th>Step</th><th>Temperature</th><th>Time</th><th>Cycles</th></tr>
<tr><td>Initial Denaturation</td><td>98°C</td><td>30"</td><td>1</td></tr>
<tr><td>Denaturation</td><td>98°C</td><td>7"</td><td rowspan="3">35</td></tr>
<tr><td>Annealing</td><td>58°C</td><td>25''</td></tr>
<tr><td>Extension</td><td>72°C</td><td>50''</td></tr>
<tr><td>Final Extension</td><td>72°C</td><td>5'</td><td>1</td></tr>
<tr><td>Hold</td><td>4°C</td><td>Hold</td><td>∞</td></tr>
</table>
</td></tr>
<tr><td>SpSULTR3;5 Amplification</td><td>
<table>
<tr><th>Name and Concentration</th><th>µL</th><th>Final Concentration</th></tr>
<tr><td>PCR grade H20, NA</td><td>13.5</td><td>NA</td></tr>
<tr><td>5X Phusion HF Buffer</td><td>5</td><td>1X</td></tr>
<tr><td>dNTP Mix, 2 mM</td><td>2.5</td><td>200 µM</td></tr>
<tr><td>Forward Primer, 10 µM</td><td>1.25</td><td>0.5 µM</td></tr>
<tr><td>Reverse Primer, 10 µM</td><td>1.25</td><td>0.5 µM</td></tr>
<tr><td>Phusion DNA Polymerase</td><td>0.5</td><td>1.0 units/25uL PCR</td></tr>
<tr><td>Template, 25 ng/µL</td><td>1</td><td>1 ng/µL</td></tr>
</table>
</td><td>
<table>
<tr><th>Step</th><th>Temperature</th><th>Time</th><th>Cycles</th></tr>
<tr><td>Initial Denaturation</td><td>98°C</td><td>30"</td><td>1</td></tr>
<tr><td>Denaturation</td><td>98°C</td><td>7"</td><td rowspan="3">35</td></tr>
<tr><td>Annealing</td><td>66°C</td><td>25''</td></tr>
<tr><td>Extension</td><td>72°C</td><td>50''</td></tr>
<tr><td>Final Extension</td><td>72°C</td><td>5'</td><td>1</td></tr>
<tr><td>Hold</td><td>4°C</td><td>Hold</td><td>∞</td></tr>
</table>
</td></tr>
</table>

Table A1.3. DNA digestion protocol used in Chapter 2 experiments.

Step	Details
(1) Mix reagents	• 38.5 µL H_2O • 5 µL 10X NEB CutSmart buffer • 5 µL of 200 ng/µL plasmid vector (1 µg total DNA) • 1.0 µL NEB PacI (10 units) • 0.5 µL NEB EcoRI-HF (10 units)
(2) Incubate reaction	15 minutes, 37°C

Table A1.4. Ligation protocol used in Chapter 2 experiments.

Step	Details
(1) Mix reagents	• Vector DNA • Insert DNA (3:1 ratio of insert to vector) • 2 µL 10X NEB Ligase Buffer • 0.5 µL NEB T4 DNA Ligase • H_2O to a total of 20 µL
(2) Incubate reaction	16 hours, 16°C

Table A1.5. Lithium acetate transformation protocol used in Chapter 2 experiments.

Step	Details
Grow initial yeast culture	Inoculate 3x5 mL YPD broth (per transformation) with yeast in 15 mL culture tubes. Grow at 30°C shaking at 200 rpm for 16 hours.
Measure OD_{600}	OD_{600} should be near 1.0.
Grow larger culture	Dilute to an OD_{600} near 0.2 in 50mL fresh YPD broth. Grow at 30°C shaking at 200 rpm until OD_{600} reaches 0.6-0.8. This takes approximately 4-6 hours.
Harvest and wash cells	Spin cultures at 3000 G for 5 minutes. Re-suspend in 2.5 mL T/E. Spin again. Re-suspend cultures in 2.5 mL T/E with LiAc. Spin again. Re-suspend in 500µL T/E with LiAc.
First incubation	Shake at 200 rpm for 1 hour at 30°C.
Plasmid addition	Divide cells into 100 µL aliquots and add 1-5 µg of plasmid to each.
Second incubation	Incubate for 30 minutes at 30°C.
Third incubation	Add 700 µL PEG solution and incubate for 30 minutes at 30°C.
Heat shock	Incubate for 5 minutes at 42°C.
Harvest cells	Centrifuge for 5 seconds at 14000 rpm and re-suspend in 500 µL T/E. Re-spin for 5 seconds at 14000 rpm and re-suspend in 100 µL H2O.
Select for transformants	Plate onto SD -Ura +Dex (2%) agar media to check for positive transformants.

Table A1.6. Final polypeptide sequences for SpSULTR2;1 and SpSULTR3;5 with highlighted ambiguous leucine/isoleucine in SpSULTR3;5.

Name	Amino Acid Sequence
SpSULTR2;1	MKERDSESFESLSQVLPNTSNPAHMIQMAMANSAGSSAAAPAGQDQLDRSKWLLDCPEPPSPWHELKS QVKESLLTKAKKFKSLRKQPLPKRILSILQAVFPIFGWCRNYKLTMFKNDLMAGLTLASLCIPQSIGYATLAKLD PQYGLYTSVVPPLIYALMGTSREIAIGPVAVVSLLISSMLQKLIDPETDPLGYKKLVLTTTFFAGIFQASFGIFRL GFLVDFLSHAAIVGFMGGAAIVIGLQQLKGLLGINNFTTNTDIVSVLRAVWRSCQLQWSPHTFILGCSFLSFIL ITRFIGRKNKKLFWLPAIAPLISVVVSTLMVFLTKADEHGVKTVRHIKGGLNPISVNDLEFNTPHLGHIAKIGVI VAVVALTEAIAVGRSFAGIKGYRLDGNKEMVAIGFMNVIGSFTSCYAATGSFSRTAVNFAAGCETAMSNIV MAVTVFVALECLTRLLYYTPIAILASIIISALPGLIDINEAIHIWKIDKLDFLALVGAFFGVLFGSVEIGLLAAVVISF AKIILISIRPGIETLGRMPGTDIFADTDQYPMSVKTPGVLIFRVKSALLCFANASFIVERIMGWINEEEEDDENT MSNAKRKILFAVLDMSNLINVDTSGITALVELHNNLIQNGVELVIVNPKWHVIHKLNQAKFISKIGGKVYLTI GEALEACFGLKV
SpSULTR3;5	MESVRTSSSSSPKRRGVNFSAPRSFFVKFKSKCKDTFFPDDPFKPISQEPNGLIKTKKTLEYFVPIFEWLPKYNL QKLRYDVLAGITITSLAVPQGISYANLASIPPIIGLYSSFVPPFVYAVLGSSNTLAVGTVAACSLLIAETFGEDML KKDPNLYLHLIFTSTFITGVFQFALGFFRLGMLVDFLSHSTITGFMGGTAIIILLQQLKGVFGIVHFTHKTDVVS VLHALFTHRDEWKWQSAVVGICFLIFLQSTRYIKKIKPKLFWVSAMGPMVVVLVGCLVAYLVKGTEHGIQT VGPLKKGLNPPSIQYLTFDAKYLPLVFKAGIVTGLIAMAEGIAIGRSFAVIKNEQTDGNKEMIAFGLMNIIGSF TSCYLTTGPFSKTAVNYNAGTKTPMSNVVMGICMMLVLLFLAPLFSYTPLVGLSAIIMSAMLGLIDYEEMYH LFKVDKFDFLVCMSAFFGVSFLSMDYGIIISVGFSVVRALLYVARPSTCKLGRIPNSDIFRDIEQYPAAEEMLGY VILQLGSPIFFANSTYVRERILRWIRDEPEGVEFLLLDLSGVSSVDMTGMETLLEVRRMLGSKGIKMVIINPRF EVLEKMMLSHFVEKIGKEYVFLSIDDAVQACRFNLSTAKPEPCT

Table A1.7. Media recipes used in Chapter 2 experiments.

Media Type	**Media Recipe**
LB (Lysogeny Broth) Media	1. Add 500 mL deionized water to beaker. 2. Add 25 grams LB powder. For plates, also add 16 g agarose. 3. Add DI water up to 1 L total volume. 4. Aliquot as desired into bottles, loose-capped. Autoclave for 45 min at 121°C. 5. Cool to 55°C in a water bath. 6. For selective media, add 1 mL of 1000x concentrated ampicillin stock (50mg/mL in 50% ethanol). Stir. 7. Pour into plates for solid media.
YPD (Yeast Extract + Peptone +Dextrose) Media	1. Add 500 mL deionized water to beaker. 2. Add 10 g yeast extract, 20 g peptone and 20 g dextrose with stirring until dissolved. For plates, also add 16 g agarose. 3. Add DI water up to 1 L total volume. 4. Aliquot as desired into bottles, loose-capped. Autoclave for 45 min at 121°C. 5. For plates, pour immediately after autoclaving.
SD (Synthetic Defined) Media	1. To a sterile 1 L bottle, add the following sterile components: a. 100 mL 10x yeast nitrogen base with ammonium sulfate b. Carbohydrate source: i. 100 mL 20% Dextrose for standard medium OR ii. 100 mL 20% galactose and 50 mL 20% raffinose for induction medium c. 10 mL 100x amino acid dropout solution (2 mg/mL adenine, 3 mg/mL leucine, 2 mg/mL histidine, 2 mg/mL tryptophan, 3 mg/mL lysine) 2. Add autoclaved DI water up to 1 L total volume.